



Robust Automated Driving in Extreme Weather

Project No. 101069576

Deliverable 3.2

Reference dataset of measured weather characteristics

WP3 – Validated sensor and sensor noise models for synthetic environments

Authors	Yuri Poledna (THI), Maikol Funk Drechsler (THI), Leticia Cristófoli Duarte (THI), Pierre Duthon (CE), Eric Henriksson (Repli5), Amine Ben Daoued (CE), Pak Hung Chan (WMG), Valentina Donzella (WMG)
Lead participant	THI, CE
Delivery date	21 May 2024
Dissemination level	Public
Type	DATA – data sets, microdata, etc

Version 03



Co-funded by the European Union. Views and opinions expressed are however those of the author(s) only and do not necessarily reflect those of the European Union or European Climate, Infrastructure and Environment Executive Agency (CINEA). Neither the European Union nor the granting authority can be held responsible for them. Project grant no. 101069576.

UK participants in this project are co-funded by Innovate UK under contract no.10045139.

Swiss participants in this project are co-funded by the Swiss State Secretariat for Education, Research and Innovation (SERI) under contract no. 22.00123.

Revision history

Author(s)	Description	Date
Yuri Poledna (THI), Pierre DUTHON(CE), Leticia Cristófoli Duarte (THI)	Draft deliverable	21/07/2023
Eric Henriksson (Repli5)	Revision 1	13/11/2023
Yuri Poledna (THI)	Post Processing after Rev.1	14/11/2023
Amine Ben Daoued (CE)	Revision 2	24/11/2023
Maikol Funk Drechsler (THI) ,Yuri Poledna (THI), Pierre Duthon (CE), Pak Hung Chan (WMG), Valentina Donzella (WMG)	Final version (v01)	11/01/2024
Eren Aksoy (HH)	Final check	12/01/2024
Andreia Cruz (accelCH)	Formatting and formal check	28/02/2024
Yuri Poledna (THI), Pierre Duthon(CE)	Added Snow effects on 2.5, and 3.3.2. Added limited scope to executive summary methodology. Added metions regarding wind in 3.1.4 and conclusion. (v02)	08/05/2024
Mario Ceccarelli (accelCH)	Logo & acknowledgement update	21/05/2024

Contents

List of Figures	5
List of Tables	5
Partner short names	7
Abbreviations	7
Executive summary	9
Objectives	9
Methodology and implementation	9
Outcomes	9
Next steps	9
1 Introduction	10
2 Methodology	11
2.1 Test-Sites	11
2.1.1 THI CARISSMA Outdoor Proving Ground	11
2.1.2 CE Proving Ground	12
2.2 Evaluated Targets	14
2.3 Rain Validation	17
2.3.1 Preliminary analysis of the sprinklers	18
2.3.2 Synthetic outdoor rain	18
2.3.3 Indoor Rain Validation	19
2.3.4 Indoor and outdoor synthetic rain comparison	20
2.3.5 Outdoor validation with real rain data	20
2.4 Fog Validation	20
2.5 Snow Collection	21
2.6 Sensor Setup	23
2.6.1 Sensor Calibration	23
2.7 Test Suites	24
2.8 Data Structure	24
3 Results	27
3.1 Rain validation and evaluation in the dataset	27
3.1.1 Individual Sprinkler analysis	27
3.1.2 Synthetic outdoor rain	27
3.1.3 Indoor Rain Validation	30
3.1.4 Indoor and outdoor synthetic rain comparison	33
3.1.5 Outdoor validation with real rain data	34
3.2 Fog Validation	35
3.2.1 Macroscopic fog validation: MOR	35
3.2.2 Microscopic fog validation: DSD	35
3.3 Data Visualization	37

3.3.1	Data collected in controlled environments	37
3.3.2	Data collected with snow in Puy de DOME	39
3.4	Dataset Availability.....	40
4	Conclusion	41
	References.....	42
	Appendix A. Actor position in the THI proving ground using RTK coordinates.....	44
	Appendix B. THI CARISSMA Test Suite.....	46
	Appendix C. CE test suite	53
	Appendix D. Disdrometer Location CE.....	66
	Appendix E. Disdrometer Location THI.....	68
	Appendix F. Measured Fog MOR for each test.....	70

List of Figures

Figure 1 Complementary CE and THI capabilities (not to scale)	10
Figure 2 CARISSMA outdoor test facilities, top view.....	11
Figure 3 THI rain sprinklers	11
Figure 4 SAPOS RTK.....	12
Figure 5 THI Target Location.....	12
Figure 6 The PAVIN platform scheme	13
Figure 7 CE target location at night	14
Figure 8 CE target location at day	14
Figure 9 Targets measured reflectivity.	17
Figure 10 Setup of the outdoor facility for the generation of the three synthetic rain intensities, sensor referenced. [6]	18
Figure 11 Data collection with the square meter method.	19
Figure 12 Sensor position during the indoor calibration measurement in the PAVIN platform.	20
Figure 13 Puy-de-Dome sensor location for snow collection	21
Figure 14 LiDAR RADAR and camera installation	21
Figure 15 Disdrometer installation.....	21
Figure 16 Dataset sensor setup.....	23
Figure 17 THI CARISSMA folder structure.....	25
Figure 18 CE Folder Structure.....	26
Figure 19 Rain intensity measurements for both sprinkler types with the square method [6].....	27
Figure 20 The three intensities of synthetic rain DSDs measurements at the THI outdoor facility [6]	27
Figure 21 Synthetic rain DSDs measurements at the THI outdoor	28
Figure 22 Intensity heat map of synthetic rain at THI outdoor facility.....	29
Figure 23 Rain intensity measured by the scale method at different points on the PAVIN platform for the four target settings.....	31
Figure 24 Average rainfall rate (continuous line) and spatial standard deviation (dashed line) recorded by the scales method as a function of the target setting value, in the PAVIN platform.	32
Figure 25 Measured and theoretical DSD obtained in the PAVIN platform, for the four simulated rainfall settings. .	32
Figure 26 DSDs of real rain in comparison with CARISSMA synthetic data	34
Figure 27 MOR measured as a function of target MOR during all tests (89 fog tests in total).....	35
Figure 28 Fog Droplet Size Distributions during ROADVIEW testing	36
Figure 29 Point cloud visualization	37
Figure 31 Dataset collected thermal camera image.	37
Figure 30 Dataset collected RGB camera image.	38
Figure 32 Lidar point cloud with snow	39
Figure 33 Landing Page REHEARSE Website Layout	40

List of Tables

Table 1 Rain amount and maximum testing distance at the THI outdoor proving grounds	12
Table 2 Targets used for the dataset.....	14
Table 3 Target sizes	16
Table 4 Parameters names and values to auto classify the snow	22
Table 5 Example description from the test suite.....	24
Table 6 Rain intensity measurements – CARISSMA outdoor test facility	30
Table 7 Rain intensity calibration at CE Pavin fog and rain indoor test facility	31
Table 8 DSD calibration at CE Pavin fog and rain indoor test facility.....	33
Table 9 Rain intensity measurements – CE Pavin fog and rain indoor test facility	33
Table 10 Rain of number of drops between CARISSMA rain facility and real rain	34
Table 11 Log-normal coefficients obtained using the method in [18].	36
Table 12 Images from the Puy de Dome data collection.....	39
Table 13 Sprinkler location in RTK coordinates and sensor referenced locations.	44
Table 14 CARISSMA test suit.....	46

Table 15 CE test suit53
Table 16 CE Disdrometer Location66
Table 17 THI Disdrometer Location.....68

Partner short names

THI	Technische Hochschule Ingolstadt
CE	Centre d'études et d'expertise sur les risques, l'environnement, la mobilité et l'aménagement
WMG	The University of Warwick
RISE	RISE Research Institutes of Sweden AB
Repli5	Repli5 AB

Abbreviations

ADAS	Advanced Driver Assistance Systems
AI	Artificial Intelligence
ASAM	Association for Standardization of Automation and Measuring Systems
AV	Automated Vehicle
CARISSMA	Center of Automotive Research on Integrated Safety Systems and Measurement Area
D	Deliverable
DAC	Direct Attached Copper
DSD	Droplet Size Distribution
EU	European Union
FLIR	Forward Looking Infrared
HEU	Horizon Europe
LiDAR	Light detection and ranging
M	Month
MDPI	Molecular Diversity Preservation International
MEMS	Micro-electromechanical systems
MOR	Meteorological Optical Range
MS	Milestone
NCAP	New Car Assessment Program
ODD	Operational Design Domain
OSI	Open Simulation Interface
PAVIN	(Intelligent Vehicle Platform of Auvergne region)
RADAR	Radio Detection and Ranging

RCS	RADAR Cross Section
RGB	Red, Green, and Blue
RMSE	Root Mean Square
ROS	Robotic Operating System
RTK	Real-time kinematic
RVIZ	ROS Visualization
SFP	Small form-factor pluggable
SWIR	Shortwave infrared
WMO	World Meteorological Organization
WP	Work Package
XIL	Everything-in-the-loop

Executive summary

Objectives

Simulation has become an important part of automated vehicle development. For there to be an accurate simulation, appropriate sensor models with a sufficient level of accuracy are required. The ROADVIEW project produces a dataset with the ROADVIEW sensors setup that enables the development of said sensor models and by extension enhance the learning of AI systems during training.

Methodology and implementation

The dataset linked to this document was created to observe the effects of different weather conditions on different sensors. The utilized sensors include a RGB camera (LUCID), a FLIR Camera, a RADAR (ZF ProWave), and LiDAR's (Innoviz One and Ouster OS1). The recording took place in the THI - CARISSMA outdoor proving ground in Ingolstadt Germany, and in the CE proving ground in Clermont Ferrand, France. The measurements were made in 3 different weather conditions (rain, clear weather, and fog); each at different intensities. Reflection effects due to adverse weather conditions are not considered, due to the scope of this task. The amount of rain was also measured and calibrated using 3 different methods, Liters per square meter, drop shape and amount, and direct weather measurement. Tests were made considering 3 EuroNCAP targets (adult male, bicycle model, and balloon car) and calibrated targets for each sensor (corner reflector for RADAR, calibration board for camera, and reflective surfaces for LiDAR). These tests were carried out during both daytime and nighttime. The positions of all involved actors were measured to establish a reliable ground truth. Sensor calibration was carefully considered and is also provided. A second data collection was made on the Puy-de-Dôme in Clermont Ferrand, to specifically capture the snow effects. This report is limited to the weather effects of snow, rain, fog, and clear weather.

Outcomes

This work provides an important contribution to both the academic community and the ROADVIEW project by contributing to the development of sensor models and denoising algorithms by leveraging annotated data taken with real sensors under adverse weather conditions in a controlled environment.

Next steps

This deliverable provides WP3, WP4, and WP5 with data that enables the production of sensor models, controllers and denoising algorithms based on the provided data, which can be used for both training and modelling purposes. This work can be integrated with labelling work to increase its usefulness regarding a broad range of works.

1 Introduction

The project ROADVIEW uses the V Methodology to implement its algorithms. This implies that to develop and validate algorithms in this project it is required to do simulation. For a simulation to be close to its reality counterpart, the XIL (everything-in-the-loop) methodology can be employed. For the XIL environment to be able to minimize the simulation-to-reality gap, one of the requirements is to have the sensor's noise model.

The importance of closing the simulation-to-reality gap is noted by authorities such as seen in [1], where the German Ministry has underlined the importance of testing algorithms using simulations that reflect as many of the aspects that define reality as possible. An example of a method to lower this gap is presented in [2] where a camera is seen in the simulation loop in a Hardware in the Loop (HIL) environment. Simulation provides the ability to quickly set up different kinds of safety-critical scenarios, avoiding the large amounts of down-time that would be involved in setting these up in the real world.

The ROADVIEW project tackles the requirement of a low simulation-to-reality gap in many ways. One of them is by generating sensor noise models. The creation of these noise models requires a dataset comprised of data from the sensors that will be utilized in the XIL environment. As the goal of ROADVIEW is to create an algorithm robust against adverse weather conditions, the models must be created to replicate these conditions. Therefore, this work discusses the creation of a dataset that will support the development of the sensor models at a later stage. The dataset requires different distances (from close to far), and different weather conditions (ranging from clear to harsh). The data collection for this work was made in the CARISSMA and CE PAVIN proving Ground, as they have complementary abilities regarding synthetic rain generation. Additionally, CE has fog generation capabilities. As shown in Figure 1, CE (light blue in the figure) can produce more rain but at closer distances compared to CARISSMA (dark blue in the

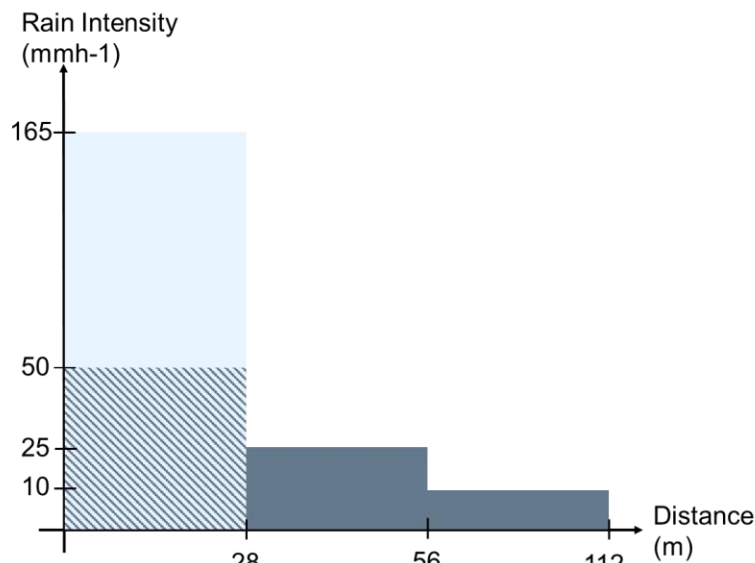


Figure 1 Complementary CE and THI capabilities (not to scale)

figure), where the size of the test track is larger, but the intensity of the produced rain is more limited.

Figure 1 shows the complementary work made in CE and THI facilities. The hashed area represents the limited overlap between the capabilities of these facilities and comes to show the importance of performing tests with different qualities in both.

This work is separated in 3 main chapters in this report. This work starts with a chapter that discusses the work's methodology. A chapter on the results of this work is presented next. Finally, the key conclusions of the performed work are explained, and the feed-forward nature of this work is demonstrated.

2 Methodology

This chapter describes the methodology utilized to produce this dataset. It is divided into 5 sections which describe the five main points of this work. Section 2.1 starts with the characterization of the test sites. Section 2.2 then evaluates the utilized targets. Next, section 2.3 discusses the rain validation methodology, which leads to the sensor definition in section 2.6. Finally, this chapter finishes with a brief description of the data structure used in the proposed dataset in section 2.7.

2.1 Test-Sites

This section describes both proving grounds used in this work, THI and CE, and their peculiarities.

2.1.1 THI CARISSMA Outdoor Proving Ground

The CARISSMA outdoor test facilities are as displayed in Figure 2 . They are comprised of an 210 m long acceleration zone (light grey area Figure 2) and a 60 m x 70 m dynamic area (dark blue Figure 2). The maximum speed is of 100km/h.



Figure 2 CARISSMA outdoor test facilities, top view

The THI part of the generated dataset in this task was executed in the acceleration zone of the THI CARISSMA outdoor facilities. This facility also provides rain capabilities using 20 water sprinklers, as seen in Figure 3.



Figure 3 THI rain sprinklers

As there is a limited number of these sprinklers, their disposition changes the water amount in the desired area. Table 1 illustrates the amount of rain that the facility can provide in relation to the distance on the X-axis of the acceleration zone. Appendix A provides the number of sprinklers and their exact position for each rain intensity.

Table 1 Rain amount and maximum testing distance at the THI outdoor proving grounds

Rain amount (mm/h)	Distance (m)
10	112
25	56
50	28

2.1.1.1 THI CARISSMA Outdoor Ground Truth Data Generation

The ground truth generation was made using the RTK system available at the CARISSMA facility. The measurement method was based on the use of a SP80 GNSS receiver, providing accuracy levels of up to 2 cm. This equipment was used for the generation of locational ground truths. Figure 4 shows the SP80 SAPOS RTK used for the collection of data related to the location of the ground truths.



Figure 4 SAPOS RTK

2.1.1.2 THI CARISSMA Outdoor Target Location

In the CARISSMA OUTDOOR proving ground measurements were made at 4 different locations relative to the sensor: 27 m, 55 m, 82 m, and 109 m.

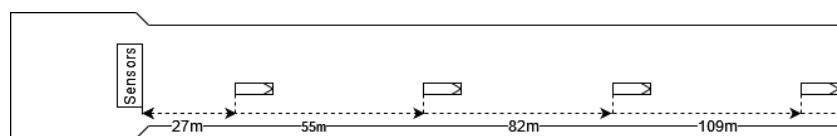


Figure 5 THI Target Location

Figure 5 shows each of the 4 positions. In each of these positions, during daytime testing, the target was positioned in 3 different orientations, 0°, 45° and 90°. During nighttime testing it had only one orientation, 0°. Where 0° is with the front of the target pointing away from the sensor.

2.1.2 CE Proving Ground

CE's PAVIN (Intelligent Vehicle Platform of Auvergne region) fog and rain platform is a unique testing facility capable of generating controlled fog and rain at a significant volume (Figure 6) [3] [4]. This platform is operated by the ITS research team of CE, a French public agency attached to the Ministry of Ecological Transition, which guarantees its independence, confidentiality, and neutrality.

The platform is 30 m long, 5.5 m wide and 2.20 m high. This volume allows to reproduce realistic road scenarios, including vehicles, pedestrians, and road equipment such as signs, road markings or other urban furniture elements.

These scenarios can be performed under night or day conditions, with or without street lighting. It is also possible to set up reference tests with calibrated targets in reflectance and thermal black bodies. Also, the tests performed in the platform can be associated with complementary measurements with scientific equipment provided by CE such as cameras (luminance, SWIR, thermal etc.) or a spectroradiometer.

The platform is mainly dedicated to the automotive (ADAS, AVs, lighting) and road (marking, traffic signs, monitoring) domains but also to other advanced domains such as railway, aeronautics, maritime, construction or military.

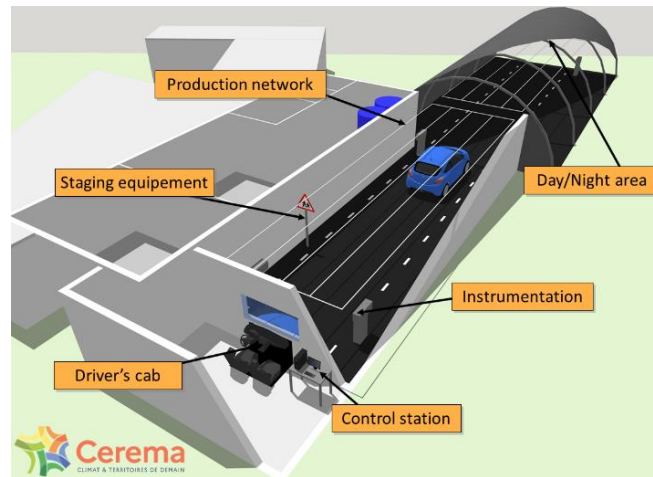


Figure 6 The PAVIN platform scheme

Within the chamber, fog and rain of varying intensities can be generated upon request. The fog density replicates the range of Meteorological Optical Range (MOR) from 10 m to 1000 m, with the Droplet Size Distribution (DSD) accurately representing continental or maritime fogs. Rain conditions can be produced with rainfall rates ranging from 10 to 180 mm/h.

The MOR [5] refers to the maximum distance (in meters) at which a calibrated object is visibly distinct from its background. The lower the MOR, the denser the fog. Fog with a MOR of 10 m is considered extremely dense and is occasionally encountered on roads.

Rain intensity [5] is characterized by the rainfall rate in mm/h, corresponding to the height of water in mm that falls on a surface area of 1 m² over a 60-minutes period. The greater the rainfall rate, the heavier the rain. A rainfall rate of 120 mm/h corresponds to severe thunderstorm peaks in Europe.

Within the platform, the average rainfall intensity is calculated as follows: the flow of water injected into the pipes is measured at the pump outlet by a flowmeter, and the production area is also known. The ratio of the two gives rain intensity in live. The pump is then controlled to maintain the desired flow rate. Calibration tests were carried out during commissioning and are carried out regularly.

2.1.2.1 CE Ground Truth Data Generation

The target location was measured using a tape measurer due to the chamber's indoor nature, and therefore its lack of strong geolocation signals.

2.1.2.2 CE Target Location

For nighttime tests 3 distances were measured, and for daytime only one. Figure 7 shows the position for the nighttime tests, where $d_1 = 10$ m, $d_2 = 19$ m, and $d_3 = 28$ m. For daytime tests the sensor location and target location

can be seen in Figure 8, which has only one target p1 at 15 m distance from the sensor setup. The daytime test was carried out in another location due to the nature of the CE proving ground.

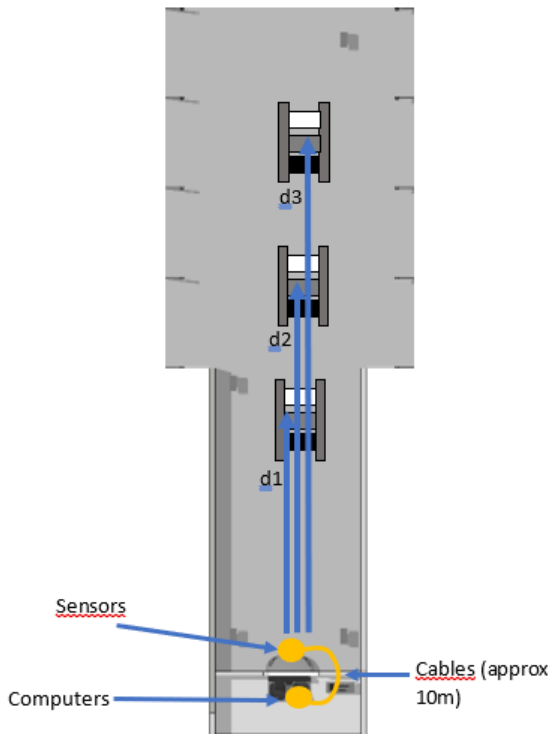


Figure 7 CE target location at night

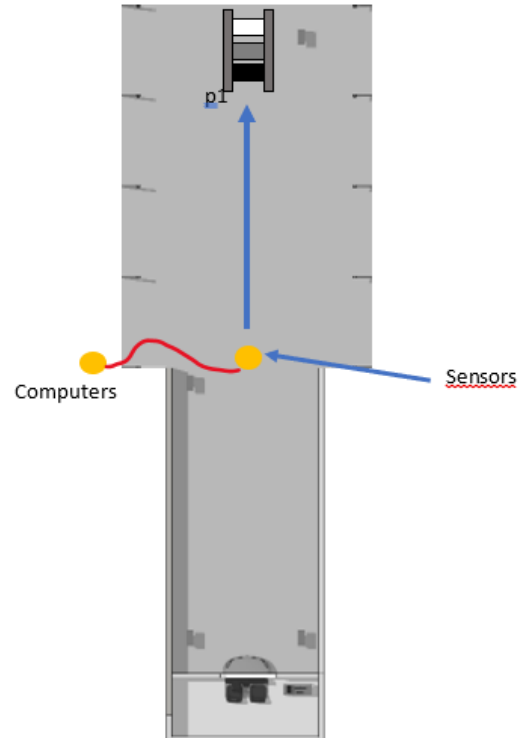





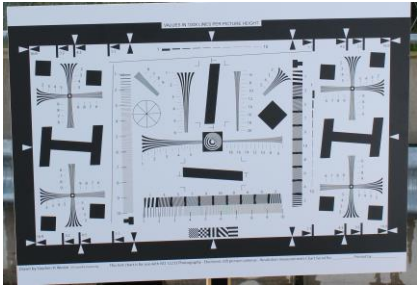

Figure 8 CE target location at day


2.2 Evaluated Targets

The utilized targets have RADAR reflection properties that reflects those of their respective real counterparts, a key aspect to ensure the resulting data is valuable for sensor modelling purposes. The portability of these targets and the possibility to place them in different locations is a valuable aspect when using them to generate a consistent dataset with a good level of variety. Moreover, 3 additional targets were used: a RADAR corner reflector with 10dBsm RCS (RADAR Cross Section), 3 LiDAR reflective targets (white, black, and self-reflective), and a camera target. These targets can be seen in Table 2.

Table 2 Targets used for the dataset.

Target Type	Image
Adult male model 4A Active PA	

Target Type	Image
Bicycle model	
Car model 4A active C2	
Camera target	
LiDAR targets	

Target Type	Image
RADAR corner reflector	

The utilized targets have the sizes described in Table 3. The camera, RADAR, and LiDAR targets have their full size described and not the size of the specific reflector.

Table 3 Target sizes

Target Type	Length (m)	Width (m)	Height (m)
Adult male model 4A active PA	0.50	0.50	1.80
Bicycle model	1.75	0.75	2.00
Car model 4A active C2	4.06	1.80	1.43
Camera target	0.10	1.50	1.80
LiDAR targets	0.50	0.50	1.80
Radar corner reflector	0.25	0.25	0.25

To have a good understanding to make the models of the sensors and targets, the reflectivity of the targets is measured in the CE facilities. This can be seen in Figure 9.

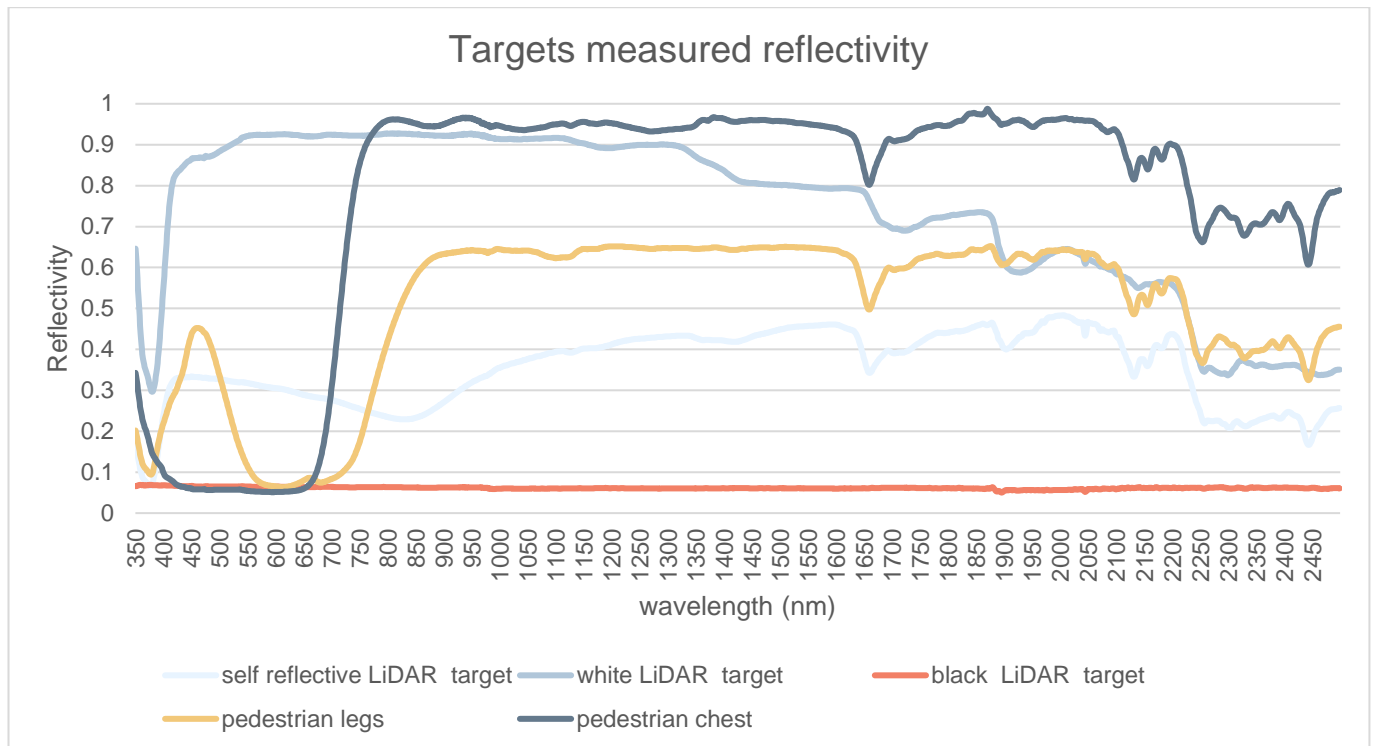


Figure 9 Targets measured reflectivity.

Figure 9 shows the reflectivity of the LiDAR targets (white, black, and self-reflective), as well as the data of the pedestrian legs and chest. Some observations to be taken from the graph are that the black target is almost perfectly consistent, with constant reflection values across the board. From the point of view of a LiDAR, the pedestrian chest can be classified as black, although it is blue in visible wavelength spectrum.

2.3 Rain Validation

For the rain validation, a 3D stereo disdrometer from Thies Clima, a portable weather station and the square meter method are utilized. The disdrometer quantifies the DSDs (droplet size distribution) of the rain, which describes a statistical distribution of the falling drop sizes, with the diameters and velocities of the respective drops. Despite its ability to provide rain intensities, it is unsuitable for application in artificial rain. Hence, to analyse and address this limitation, the concept of water volume derived from the DSDs is introduced and is predicated upon the assumption that raindrops assume a spherical form.

The “Weather HAT” weather station is equipped with mechanical sensors that operate through physical interaction with wind and rain. It utilizes magnets, reed switches, and moving parts to generate signals, which are then processed by a Raspberry Pi 4 Model B. These sensors provide measurements for wind speed, wind direction, and rain intensity.

The square meter method consists of recording the amount of collected water within a predefined time and then calculating its volume using weight and density of water. Subsequently, utilizing the recipient's surface area A the rain intensities can be computed [6].

The collected data is thus subjected to a comprehensive assessment, involving four distinct analyses that draw comparisons across three distinct environments: outdoor synthetic rain, indoor synthetic rain, and real-world rain conditions. These comparisons serve the purpose of evaluating the similarity between artificially emulated and authentic rain patterns, while also examining the efficiency of the generated rain under outdoor circumstances as compared to controlled indoor settings. Detailed accounts of each analysis are elaborated upon in the subsequent subsections [6].

2.3.1 Preliminary analysis of the sprinklers

With the purpose to understand the capabilities of the outdoor rain facility and identify the intensity distribution generated by the different systems, a preliminary test is conducted evaluating the performance of two different garden sprinklers. The evaluated equipment consists of a rotating sprinkler, with a flow of 6.88 L/min, and a spray sprinkler, with a flow of 8.90 L/min. Each of these sprinklers covers a semicircular area spanning 180 degrees, with an effective radius of 9 m. The main difference is that the rotating sprinkler has a rotating water jet that scans the actuation area, while the spray sprinkler generates a widespread waterjet in its actuation area.

For the evaluation, the volumetric quantity of water produced by each sprinkler in 30 min is measured in five distinct positions. These positions are linearly aligned with the radius of the sprinkler and spaced at 1.8 m intervals. Additionally, with the value of the volumetric quantity of water in the five positions, the square meter method is employed to compute the average of rain intensity for the sprinklers [6].

2.3.2 Synthetic outdoor rain

The disposition of the sprinklers can be seen in Figure 10 represented by triangular markers represent the positions of rotating sprinklers, serving as supplementary elements depending on the rain intensity. The yellow markers are employed throughout the entire 112 m generating 10 mm/h rain intensity. However, for the 25 mm/h intensity, rain is only generated in the first 56 m, so it uses yellow and red rotating sprinklers for that distance. Lastly, in the case of rain intensity of 50 mm/h, the green markers are introduced, while the yellow and the red markers starting from 28 m of distance are removed [6].

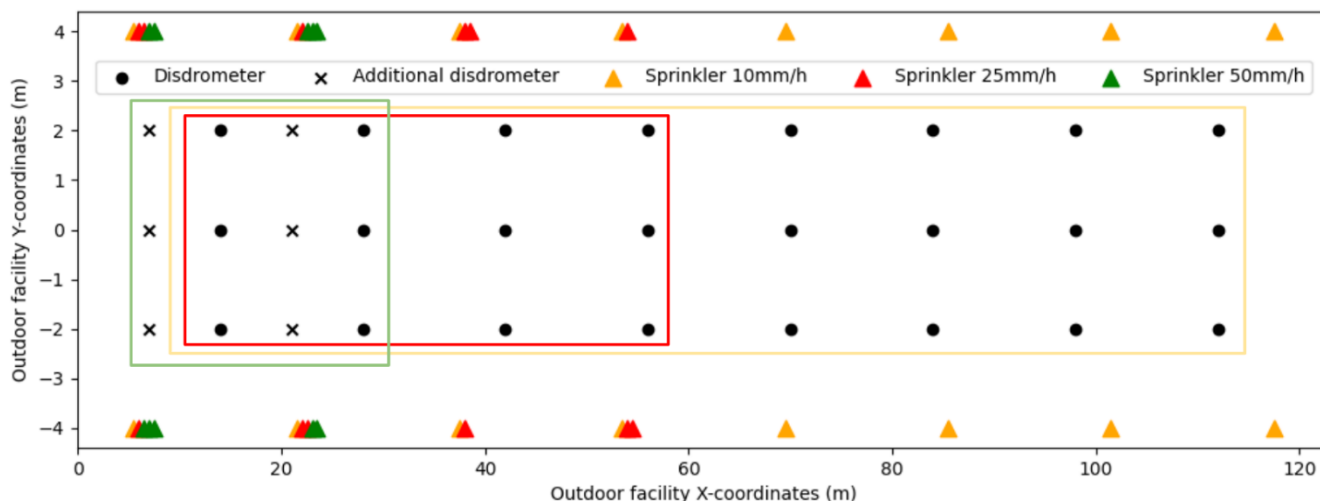


Figure 10 Setup of the outdoor facility for the generation of the three synthetic rain intensities, sensor referenced. [6]

Figure 10 includes circular markers indicating the designated positions for the disdrometer measurements, while the cross markers are exclusive measurement positions for the 50 mm/h rain. Furthermore, the square markers delineate the disdrometer zones for each intensity — yellow for 10 mm/h, red for 25 mm/h, and green for 50 mm/h. At the same location as the disdrometer, data is also collected by the Weather HAT and the square meter method. The records are collected over one minute at each point for the disdrometer and for the Weather HAT. For the square meter method, data is collected over 30 minutes, as shown in Figure 11. The disdrometer exact RTK GPS positions can be further understood in Appendix E.



Figure 11 Data collection with the square meter method.

2.3.3 Indoor Rain Validation

As part of the ROADVIEW project, tests were carried out on the PAVIN platform (CE). The aim of these tests is to create and validate noise models for degraded weather conditions. These models concern visible camera, LiDAR, and RADAR sensors, for foggy and rainy weather conditions. To validate the models, it is necessary to be certain of the conditions present in the test chamber, particularly in the case of rain. To this end, CE and THI carried out a specific calibration campaign for the rain conditions simulated on the platform. The literature shows that two parameters characterizing rainfall are particularly important: (a) rain intensity, the macroscopic parameter that corresponds to the volume of water that falls in each time period and (b) the DSD of rain, the microscopic parameter. A third parameter is important for testing under physically simulated conditions. This is rain uniformity, measured by the standard deviation of the spatial distribution of rain intensity.

As part of the ROADVIEW tests, 4 target rainfall intensities were simulated in the PAVIN fog and rain platform: 17, 50, 101, and 175 mm/h. Various sensors were used for characterization: rain buckets based on scales (square meter method) and an OTT Parsivel disdrometer. The analyses will be presented in the following order:

1. An analysis of rainfall uniformity across the platform, giving average rain intensity values for the four target settings used.
2. An analysis and characterization of the DSD for each of the simulated rainfall intensities.

Calibration tests were carried out as follows. The sensors (three balances, the Weather HAT, the OTT Parsivel and the Clima Thies) were placed successively at 12 positions in the platform, following the plan shown in Figure 12 and the order in Appendix D. For each position, the four target settings were applied for 1 minute. This represents 48 1-minute records. Each time, an initial period of rain stabilization was respected so that it remained stable during the minute of recording. During this minute, the disdrometer records the total number of drops passing in front of their measuring beam, and the scales record the evolution of the weight of water collected in the bucket. These values are then related to the physical quantities of rain intensity (expressed in mm/h) and DSD (expressed in $\text{part.m}^{-1}.\text{m}^{-3}$). This makes it possible to check the spatial uniformity of rain intensity, and to obtain the average DSD over the entire platform.

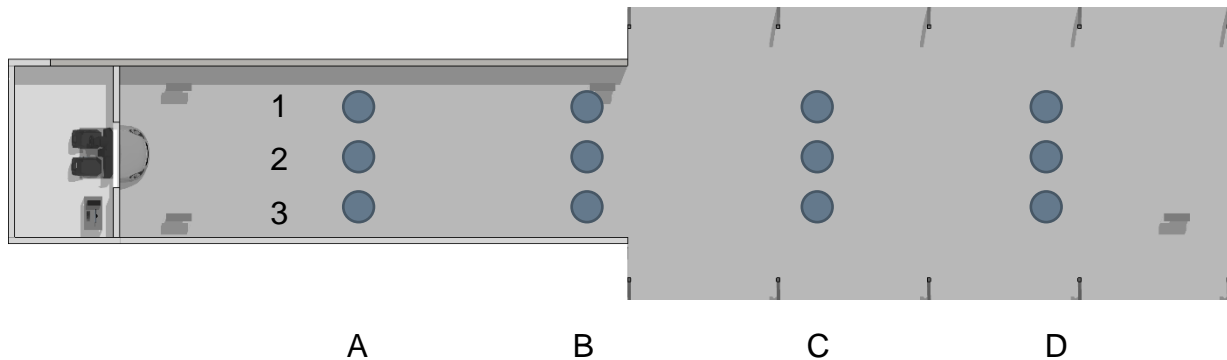


Figure 12 Sensor position during the indoor calibration measurement in the PAVIN platform.

2.3.4 Indoor and outdoor synthetic rain comparison

Data from CARISSMA and CE is examined using the square meter method and the Weather HAT, analysing the rain and wind parameters. The detailed results of these comparisons are further elaborated in the subsequent chapter.

2.3.5 Outdoor validation with real rain data

To validate if the synthetic rain exhibits similar characteristics to real rain, the disdrometer and the Weather HAT were set outdoor to collect continuous data of the environment over a period of 5 days. Subsequently, an initial processing of the data to identify the rainy periods is required. From the total amount of over 6.700 minutes of recorded data, 370 minutes are detected as rainy conditions, by observing whether the number of drops detected by the disdrometer exceeded 100.

For those files, the DSDs curves are compared with the synthetic outdoor rain data and as an evaluation method, the Root Mean Square Error (RMSE) is applied. RMSE can be conceptualized as a representation of the standard deviation characterizing the disparities between measurements and a reference curve [7].

2.4 Fog Validation

The fog tests were carried out indoors only, on the PAVIN Fog and Rain platform. Fog has already been validated from a general point of view inside the platform [8] [3]. However, additional live measurements have been carried out to obtain greater precision in the development of the noise models developed in the ROADVIEW project. It is proposed here to analyze fog by focusing separately on the macroscopic and microscopic aspects. As far as the macroscopic aspect is concerned, the MOR is used in the literature. Section 3.2.1 will therefore give a definition of the latter and show which MORs were obtained on the PAVIN platform during testing. As far as the microscopic aspect is concerned, it is DSD that is generally studied in the literature. Section 3.2.2 will therefore show the average DSDs obtained and give the results of an optimization method to obtain a law corresponding to each DSD.

2.5 Snow Collection

The CE chamber and the THI outdoor facility don't possess snow capabilities, and due to that, data was collected from the Puy-de-Dôme volcano, in Clermont Ferrand, where CE has a facility to measure weather effects. With the addition of snow, all major weather effects are covered by this dataset, Fog, Rain, and Snow. The location of the sensor installation can be seen in Figure 13.



Figure 13 Puy-de-Dôme sensor location for snow collection

During the winter of 2022 to 2023, CE collected data using the sensor suite (seen in Figure 14):

1. ZF RADAR ProWave,
2. Velodyne VLP16,
3. Canon Axis Q1656-LE Camera.



Figure 14 LiDAR RADAR and camera installation



Figure 15 Disdrometer installation

The weather effects of rain and snow were measured using the OTT Parsivel, the Vaisala PWD12 was used to measure temperature, fog, and rain or snow amount. Additionally, the WXT530 was used to measure rain and snow,

and the VS2k was used to measure the fog (seen in Figure 15). The data collection in the Puy-de-Dome was made by measuring 1 minute of the sensor data each hour.

Due to the knowledge of the weather conditions and using multiple sensors, it is possible to automatically make a classification of snow using the parameters seen in Table 4.

Table 4 Parameters names and values to auto classify the snow

Parameter Name	State
<i>Parsivel_Weather</i>	<i>[' S-', ' S', ' S+']</i>
<i>PWD12_Temperature (°C)</i>	<i><5°C</i>
<i>Parsivel_Rain intensity (mm/h)</i>	<i>>0</i>
<i>WXT530_Rain intensity (mm/h)</i>	<i>>0</i>

Note: for snow, Rain intensity is the parameter (falling water volume, in iced form)

2.6 Sensor Setup

To capture the defined static scenarios, a sensor suite was defined. This collection of sensors is defined in this section.

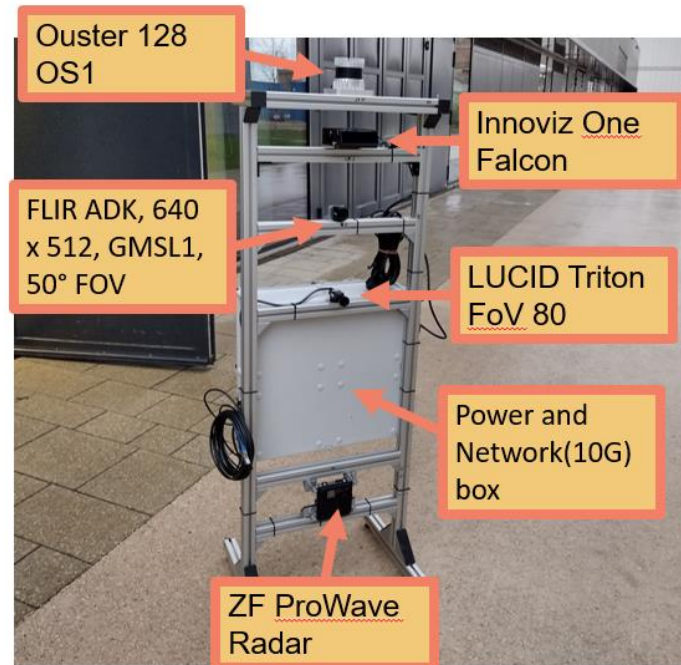


Figure 16 Dataset sensor setup

Figure 16 shows the dataset's sensor setup. From the top down, an Ouster OS1 128 channel LiDAR, followed by an Innoviz One Falcon LiDAR, a LUCID Triton Camera, and finally a ZF ProWave RADAR at the lowest position. All the data is concentrated into a 10 Gbps ethernet switch in the box that is between the ZF RADAR and the LUCID camera. This box also provides power to the sensor setup. The box outputs data to a computer a small form factor pluggable (SFP) transfer cable with 10Gbps transmission speed and a power plug that receives power.

This comprises a very complete set of sensors due to the different properties of each. There are passive sensors such as the cameras and active sensors such as the LiDAR's and RADAR's. There are two LiDAR's: one rotative and another relying on micro-electromechanical systems (MEMS). The RADAR is a 4D RADAR from ZF, which counts with the traditional 3 dimensions from a normal RADAR, distance, velocity, azimuth, and an extra dimension, the elevation. The RGB camera and the thermal camera are finally capable of fully observing the scene light spectrum.

2.6.1 Sensor Calibration

With the ground truths for the dataset usage, it is important to make the projection from 3D points to 2D pixel coordinates. This is achieved using the cameras' intrinsic calibration matrix. Such matrices were measured using a checkerboard pattern with 9x6 squares with edges of 110 mm.

The extrinsic calibration was calculated using specialized MATLAB and ROS scripts for the measurement. For there to be a guiding path, the position was measured using a total station and a metric ruler.

2.7 Test Suites

With all the required setups ready it is possible to define the scenarios that will be executed to construct this dataset. The full list of these test suites is available at Appendix B and Appendix C.

Table 5 shows a small example of what is seen in Appendix B. The first column assigns a numerical value to every test to be executed. The second column describes whether the test is to be performed during daytime or nighttime and whether it is to be held in dry or specific raining conditions. The third column describes the sprinklers, and which position they need to be in, as seen in Figure 10. The target column shows which target needs to be used, followed by its distance and angle in the following columns. The last column is an estimation on the needed time to perform the data collection and target setup.

Table 5 Example description from the test suite

Test	Description	Sprinklers	Target	Distance	Angle	Time
7.1	50 mm/h	Position 3	Pedestrian	28	0°	10
7.2				28	45°	2
7.3				28	90°	2
7.4			Bicycle	28	0°	10
7.5				28	45°	2
7.6				28	90°	2
7.7			Car	28	0°	10
7.8				28	45°	2
7.9				28	90°	2
7.10			Corner Reflector	28	0°	10
7.11			LiDAR Targets	28	0°	10
7.12			Camera Targets	28	0°	10

2.8 Data Structure

Following the test suite described in Section 2.7, a folder-based structure was utilized, which provides the base structure without elongated filenames. The data was initially recorded using the Robot Operating System (ROS) [9] environment, into rosbag. This data was then post processed into the ASAM Open Simulation Interface (OSI) [10] method for publication. The data was then compacted into tar.gz files to decrease the total amount of utilized server space and lower the amount of load on the network, and thus decrease the download time. The dataset was separated in two main parts, the THI, and the CE data collections and inside these 3 parts for the CE captures (pedestrian and bike, car, and targets) and 4 parts for the THI captures (pedestrian, bike, car, and targets).

The folder structure is fully described in Figure 17 and Figure 18.

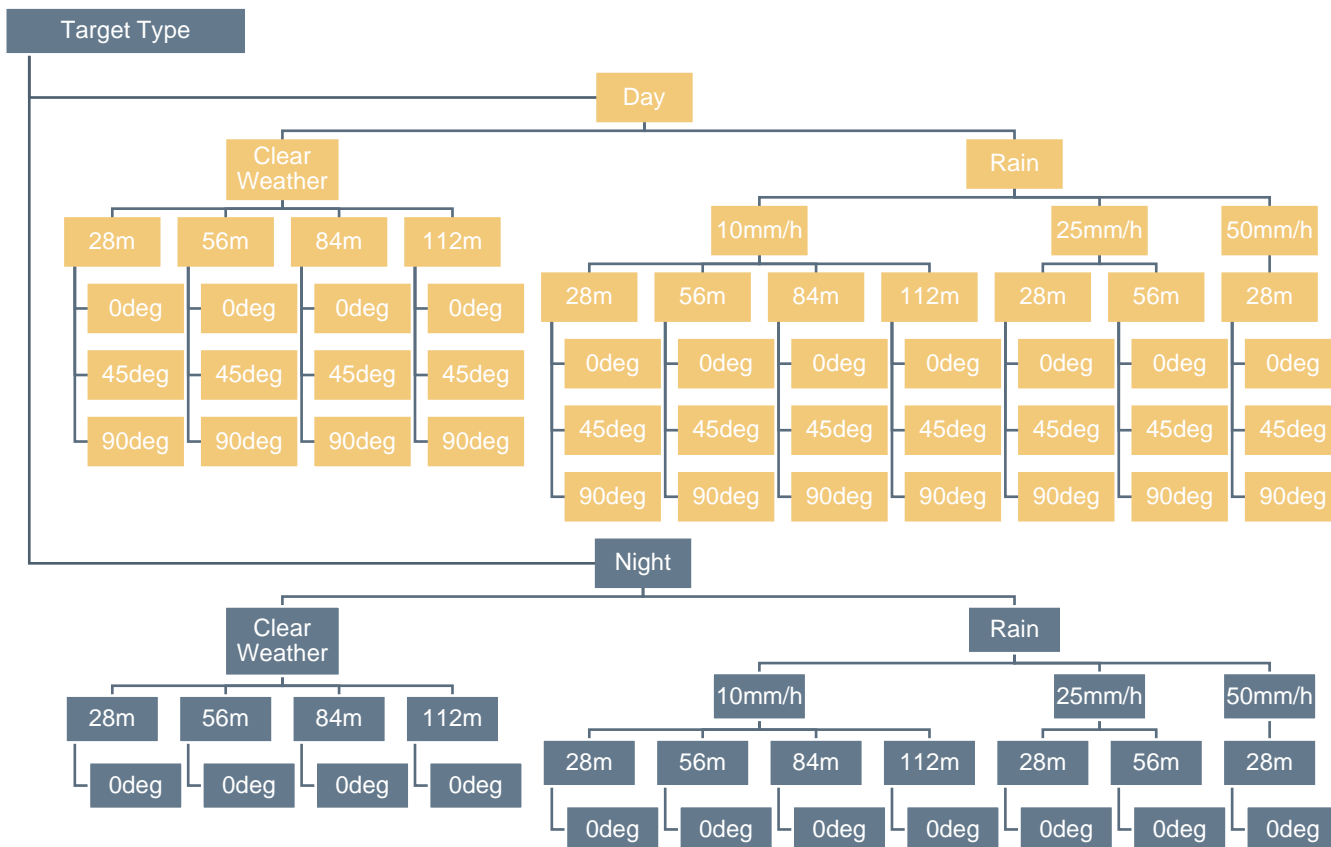


Figure 17 THI CARISSMA folder structure

As a quick guided example in Figure 17, for each type of target there is a folder, and in each of these there is a folder for nighttime and another for daytime cases. Inside each of these there are two other folders, one for clear weather and one for rainy weather. Inside the rain folder the different rain intensities can be found, and inside this folder (and the folder with clear weather) different folders for each distance. Inside each folder for each distance there are folders with the sensor names or the target angle. Though the sensor names are known, it was decided to choose more generic names for the sensors, such as the ZF ProWave RADAR became 4D RADAR and the Innoviz One LiDAR is the MEMS LiDAR.

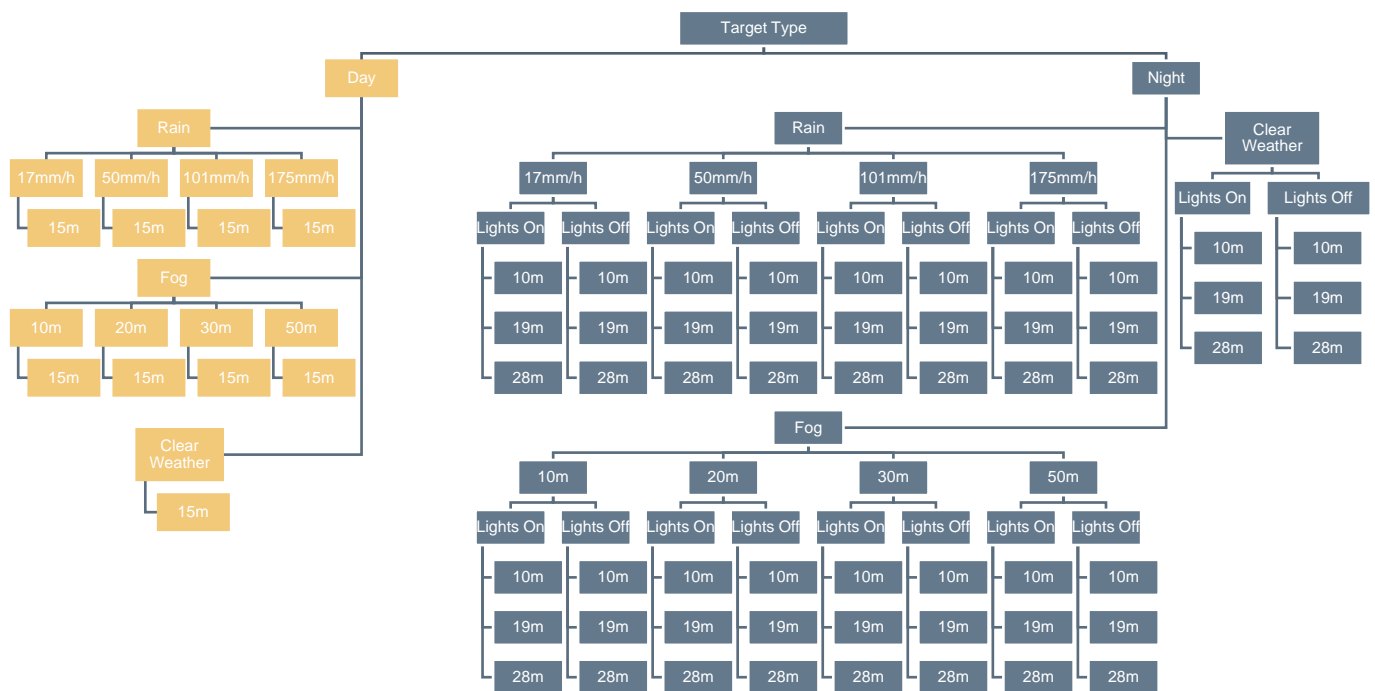


Figure 18 CE Folder Structure

Figure 18 describes the folder structure of the CE data capture. The main difference from CE to THI is that CE has lower distances and fog. The fog folders are like rain, but instead of having rain rates the folder names describe the maximum visibility in meters. The CE capture has with car lights on and off.

3 Results

This chapter is split into 3 sections: the first discusses the results of the work related to the rain tests, the second briefly demonstrates the collected data. Finally, this section is rounded up with the presentation of the website and how it was made available for publication.

3.1 Rain validation and evaluation in the dataset

This section discusses the results of the rain tests in the different test chambers. It provides an analysis of the individual sprinklers at THI, followed by the synthetic outdoor rain analysis, then a comparison of indoor (CE) and outdoor (THI) rain facilities, and finally a validation of the rain produced by the THI proving ground based on real rain data.

3.1.1 Individual Sprinkler analysis

The rain intensities of the two sprinkler types across the five measured positions are visualized in Figure 19. The spray model exhibits a higher water flow, resulting in elevated rain intensities. Conversely, water deposition from the spray model is confined only in the 1.8 m position. In contrast, it can be noticed that the rotating sprinkler displays a uniform dispersion of water droplets across its effective radius, encompassing all positions and a more linear curve. Therefore, the rotating sprinkler is chosen as the preferred option for rain generation. [6]

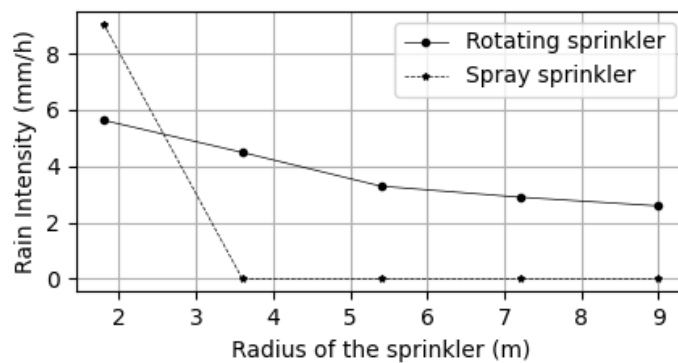


Figure 19 Rain intensity measurements for both sprinkler types with the square method [6]

3.1.2 Synthetic outdoor rain

First, the comparison of the three different rain intensities is performed. The DSDs results measured for all intensities in CARISSMA at the position $x = 28$ m and $y = 0$ m are shown in Figure 20.

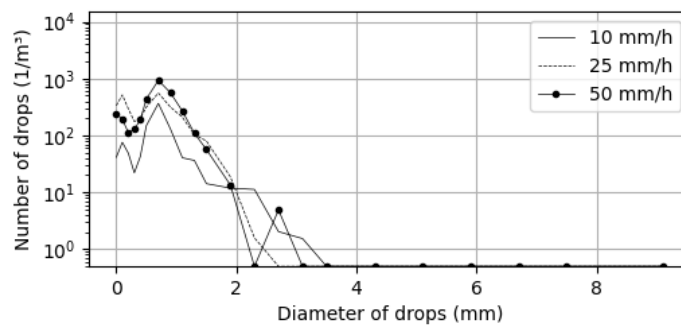


Figure 20 The three intensities of synthetic rain DSDs measurements at the THI outdoor facility [6]

It can be observed that most drops across the three curves are concentrated in a diameter range of 1 mm to 2 mm. Comparatively, occurrences of larger drops are less frequent. It is worth noting that the overall count of droplets remains relatively high, and the curves follow the same structure. The peaks are higher as the intensity grows. The outputs exhibit a coherent pattern, highlighted by the rain intensity curve of 25 mm/h that converges between the other two curves. This alignment alludes to a consistency of the measurements, in which greater rain intensities denotes a greater absolute quantity of rain drops. [6]

Furthermore, the results of all disdrometer measurements are represented in DSDs and two distinct analyses are performed:

- Consistency of the rain distribution on the longitudinal range, comparing all the X positions for one specific Y position.
- Consistency of the rain distribution on the lateral range, comparing all the Y positions for one specific X position.

Figure 21 provides an example of the 10 mm/h DSDs for the longitudinal and lateral ranges. For the longitudinal evaluation, only three distances are selected (beginning, middle and end) to facilitate the graph representation. At the longitudinal evaluation, the DSD of the 14 m has the extended area beneath the curve, so a more intense rainfall is evident. In contrast, the curve has notably fewer drops in the DSD measured in the 112 m distance. Additionally, in the lateral evaluation, the point on the right side of the test facility has a higher rainfall drops registered compared to the other lateral positions. [6]

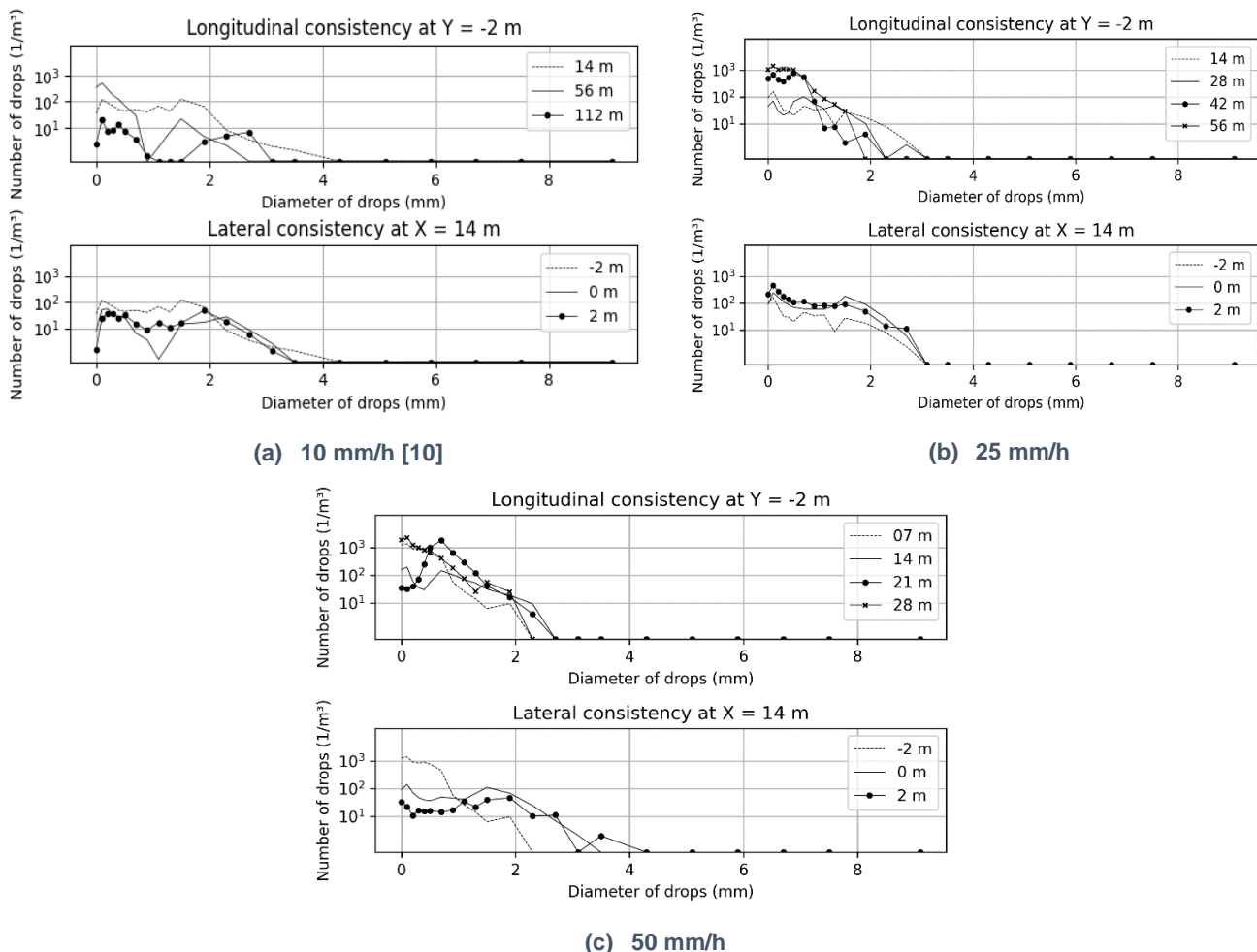


Figure 21 Synthetic rain DSDs measurements at the THI outdoor

The rain intensity values measured with the square meter method are shown in the heat map of Figure 22, considering a nominal 10 mm/h rain intensity. In the heat map, the darker blue regions represent the 14 mm/h, while the lighter regions reach values of 2 mm/h. The result indicates that the uniformity remains up to 80 m, in which the

intensity remains between 8 mm/h, and 14 mm/h. The highlight peaks of rainfall occur close to (21, -2) and (60, 2) coordinates, denoted as (X, Y). [6]

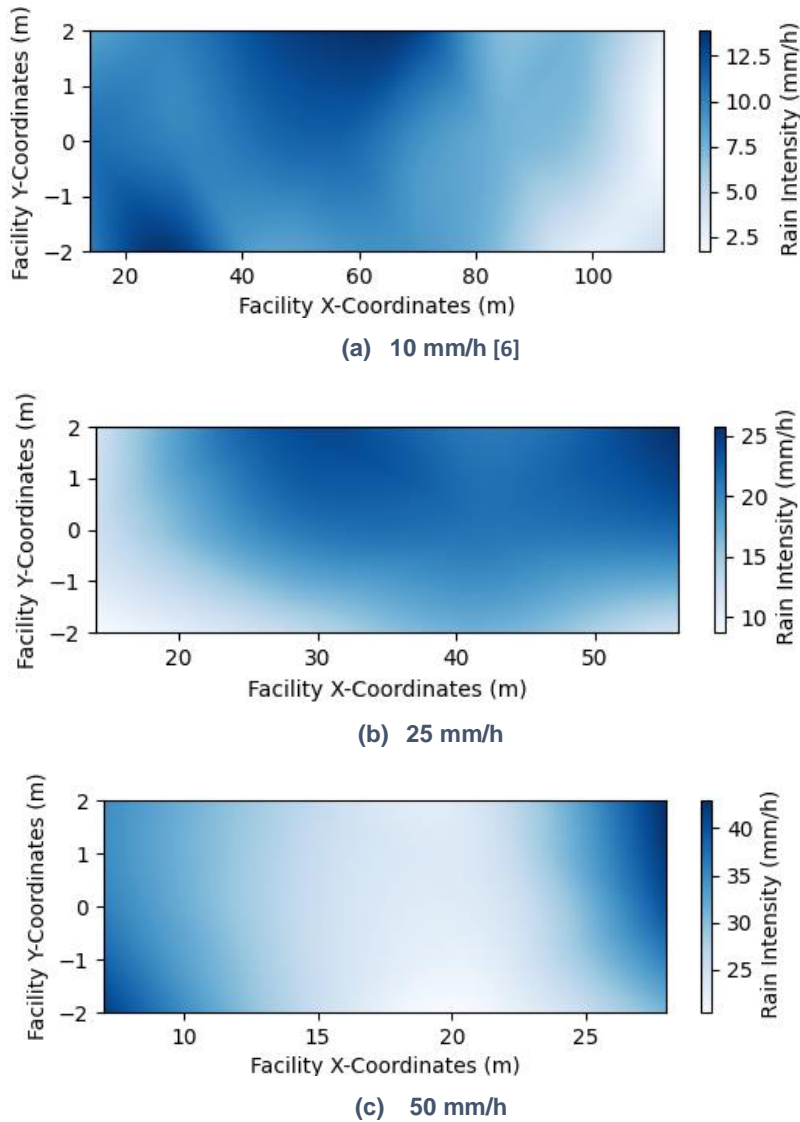


Figure 22 Intensity heat map of synthetic rain at THI outdoor facility

A notable similarity can be discerned between Figure 20 and Figure 22, as both offer analogous findings. For instance, at 112 m, an absence of drops is evident, while at 14 m, the peaks are significant at -2 m, followed by 0 m and 2 m. These trends are apparent in both images, represented differently, but handed the same outcome. This observation supports the conclusion that the square meter method aligns with the findings of the disdrometer and that there is wind interference in the tests. [6]

It is observed that uniformity is influenced by wind, particularly in the data collected at 50 mm/h. It is evident that weather conditions in outdoor, during the 50 mm/h measurement, are more extreme compared to the other intensity measurements. Table 6 provides the wind data for the three rain intensities, alongside with the rain intensity measurements average using both the square meter method and the Weather HAT station. [6]

Table 6 Rain intensity measurements – CARISSMA outdoor test facility

Nominal Intensity (mm/h)	Square meter (mm/h)	Weather HAT (mm/h)	Wind average (m/s)
10	8.7	4.9	1.3
25	17.4	16.7	1.9
50	31.2	2709.4	45.1

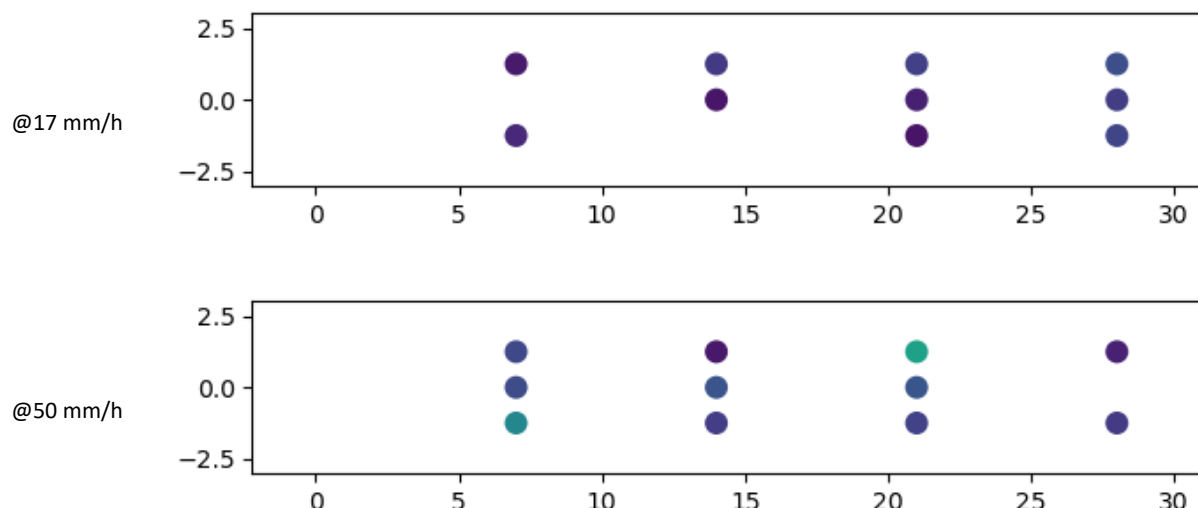
The average rain intensities align with the nominal values, considering the low intensities presented at the borders as shown in Figure 20. This phenomenon is attributed to the wind carrying the rain away from the area of interest. Nevertheless, a disparity between the two measurements’ approaches is evident in Table 6. For a wind speed of 45 m/s, the Weather HAT station is reporting 2709.4 mm/h of rain intensity, a non-realistic value [11]. Therefore, a limitation in the tipping mechanism of the Weather HAT station is identified when in contact with higher winds. This magnifies the importance of recording wind data. [6]

3.1.3 Indoor Rain Validation

The analysis of indoor tests is divided into two successive parts:

- An analysis of rainfall rate uniformity across the platform, giving average rain intensity values for the four target settings used.
- An analysis and characterization of the DSD for each of the four simulated rainfall intensities.

Figure 23 shows the rainfall intensity recorded at various points on the platform. These points have been chosen arbitrarily on a grid, without considering the distribution of rain nozzles. This ensures that the measurement is representative and as unbiased as possible. Figure 23 shows the four target intensity levels used (17, 50, 101 and 175 mm/h). Some points on the grid are missing, i.e., those for which the scales were unable to measure successfully. This happened when the rain level was not considered stable enough during the minute of measurement. As it can also be appreciated in Figure 23, the rainfall rate is relatively homogeneous along the longitudinal central axis (except near 15 m for heavy rains), which was the main criterion for designing the platform’s rainwater system. Around this axis, the rainfall uniformity is not perfect.



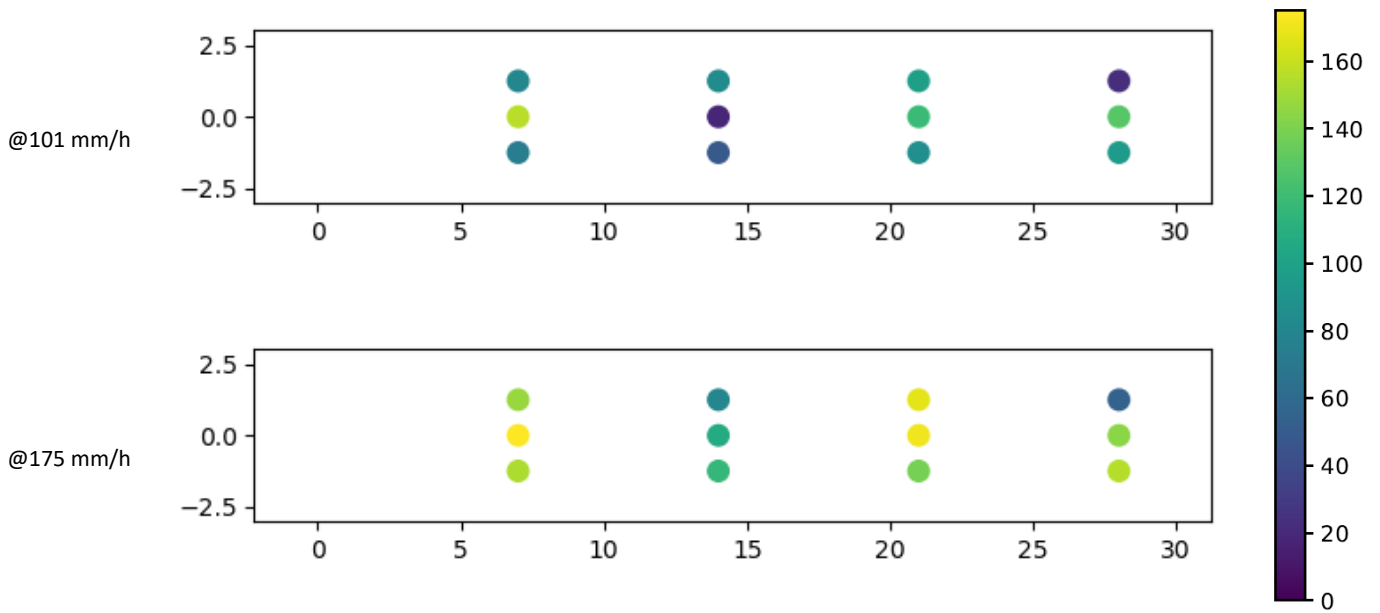


Figure 23 Rain intensity measured by the scale method at different points on the PAVIN platform for the four target settings.

To better assess the uniformity, we calculate the mean rainfall rate and its spatially standard deviation of the various measurement points (see Figure 24). The rain intensities measured by the scales method and the OTT Parsivel are less than the target values. This is due to the definition of the target value: knowing the whole surface S of the PAVIN platform, the water flow Q injected in the pipes is servo-controlled so that the ratio Q/S is close to the rain intensity target. As not all water is sprayed on the test area, and some quantity of water is sprayed on the walls, this leads to an effectively smaller rain intensity, this effect can be observed on Table 7.

Table 7 Rain intensity calibration at CE Pavin fog and rain indoor test facility

PAVIN platform setting (mm/h)	Real values calibrated by scales (mm/h)	Relative gap (%)
17	19	12
50	39	22
101	83	18
175	139	26

The second observation is that the values returned by the two sensors are consistent with each other. Measurements are taken at two different heights by the sensors: 30 cm for the scales and 120 cm for the OTT Parsivel. This shows good height homogeneity between the ground and 120 cm. We can nevertheless remark that OTT Parsivel intensity is lower than the scales method-based intensity. This underestimation of rainfall intensities by OTT Parsivel compared with those measured by rain gauge is known in the literature [12].

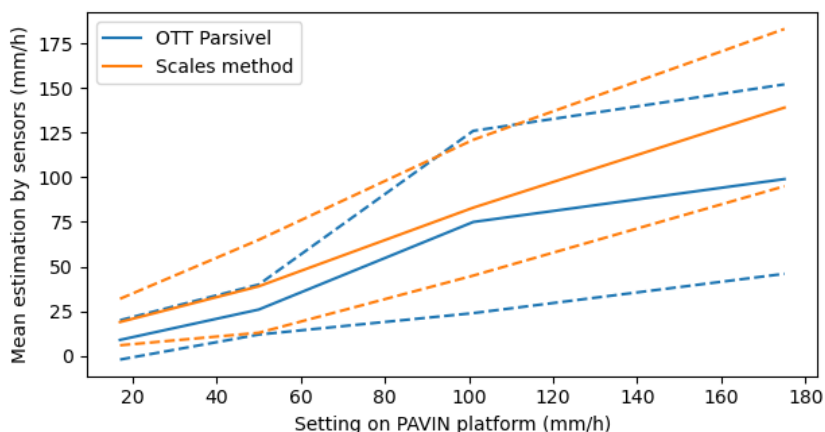


Figure 24 Average rainfall rate (continuous line) and spatial standard deviation (dashed line) recorded by the scales method as a function of the target setting value, in the PAVIN platform.

Figure 24 shows that the spatial standard deviation of rain intensity ranges monotonically between 60% for low rainfall intensities (target 17 mm/h), and 30% for high rainfall intensities (target 175 mm/h).

The second part of the analysis focuses on the DSD of rain. This parameter is crucial to rainfall models. The average DSD of the platform was measured by the OTT Parsivel sensor and normalized to match the measured rain intensity. The theoretical DSD obtained by Marshall Palmer's distribution [13] was also calculated. Figure 25 shows these two types of DSD (solid lines and dashed lines) for the four target rainfall intensities simulated on the PAVIN platform (in colour).

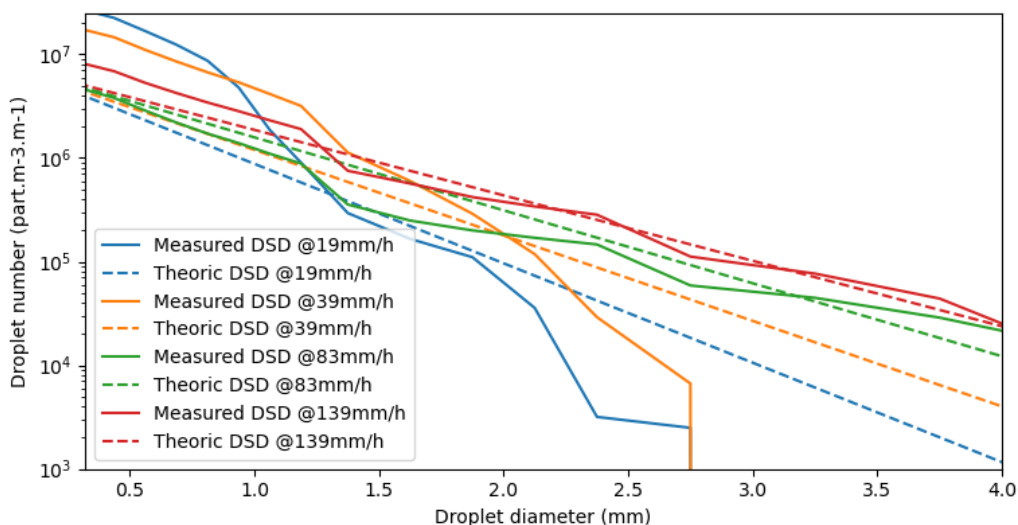


Figure 25 Measured and theoretical DSD obtained in the PAVIN platform, for the four simulated rainfall settings.

Figure 25 shows that the DSDs obtained at rainfall intensities of 19 mm/h and 39 mm/h have far too many small drops (almost 10 times more for drops smaller than 1 mm). Conversely, these DSDs lack drops over 2 mm in diameter. The DSDs for the two highest rainfall intensities (83 mm/h and 139 mm/h), on the other hand, correlate well with Marshall Palmer's law. This difference between the different DSDs stems from the rain production mechanism within the PAVIN platform. Indeed, to obtain the most natural DSDs possible, different nozzles and pressures are used. It turns out that the results obtained are best for the highest rainfall intensities (83 mm/h and 139 mm/h). For the other two rainfall intensities, the Marshall Palmer parameters need to be modified in the models if one wants to achieve similar behaviour. The parameters to be used are listed in Table 8.

Table 8 DSD calibration at CE Pavin fog and rain indoor test facility

PAVIN platform target setting (mm/h)	Real values calibrated by scales (mm/h)	Measured DSD by OTT Parsivel		Theoretical value from Marshall Palmer	
		Λ (cm-1)	N_0 (cm-4)	Λ (cm-1)	N_0 (cm-4)
17	19	41.44	1.57	22.09	0.08
50	39	32.05	0.84	19.00	0.08
101	83	13.62	0.04	16.21	0.08
175	139	12.08	0.06	14.55	0.08

Table 8 gives the average actual values to be retained in the models, rather than the target values indicated by the CE PAVIN platform.

3.1.4 Indoor and outdoor synthetic rain comparison

The data of CE PAVIN fog and rain for 4 different rain intensities are used to calculate the averages of the rain intensity from the square meter method and the Weather HAT. The results are presented in Table 9.

Table 9 Rain intensity measurements – CE Pavin fog and rain indoor test facility

Nominal intensity (mm/h)	Square meter (mm/h)	Weather HAT (mm/h)
17	22.3	8.4
50	43.2	22.3
101	82.8	242.8
175	139.3	803.6

The limited functionality of the Weather HAT station is not solely confined to wind conditions. Notably, significant deviations in values are observed for rainfall intensities surpassing 800 mm/h, even in the absence of wind.

When comparing Table 6 and Table 9, it becomes evident that the values obtained through the square meter method are approximately 20% closer to the nominal intensity in indoor conditions. This observation strongly suggests that wind does indeed have a significant impact on the test results. The wind consideration of wind may be taken into account by Task 3.5.

3.1.5 Outdoor validation with real rain data

Within the files capturing real rain events, specific instances exhibit elevated water volumes, indicating intensified rainfall during those minutes. Due to existing doubts about the reliability of Weather HAT's rain intensity measurements, utilizing its data to compare with the synthetic rain is not feasible. As a result, for a valid comparison, the total water volume for each file of the DSD is computed.

The approach involves calculating water volumes for the curves Figure 20, and subsequently selecting real rain measurements with comparable volumes. Figure 26 shows the comparison between the real rain and CARISSMA synthetic rains, based in the volume from the DSDs.

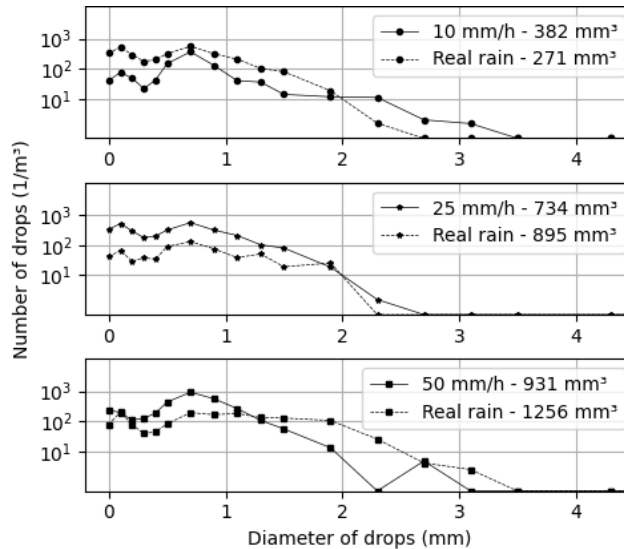


Figure 26 DSDs of real rain in comparison with CARISSMA synthetic data

The dashed lines in Figure 26 represents real rain data, revealing that the curves exhibit a similar shape in each comparable volume with the synthetic ones. The generation of the three intensities is thus acceptable. Table 10 presents the results of RSME from the curves when comparing the real rain with the synthetic rain from CARISSMA's facilities.

Table 10 Rain of number of drops between CARISSMA rain facility and real rain

Set rain amount (mm/h)	RMSE (Number of drops)
10	53.4
25	169.1
50	202.3

The curve from 10 mm/h presents the highest similarity with the real rain with a RMSE of 53.4. Additionally, as all intensities have the number of drops in the order of 1000, the RMSE are relatively small, showing an acceptable use of the proposed method for synthetic rain generation.

3.2 Fog Validation

This section focuses on the macroscopic and microscopic fog validation. This section is divided into two classes, with similar names to the observed effects.

3.2.1 Macroscopic fog validation: MOR

Fog is first characterized from a macroscopic point of view by the MOR, also known as visibility [5]. MOR is directly related to fog density. The lower the MOR, the denser the fog. In a road environment, fog is present at a MOR below 400m. The PAVIN platform can produce fog up to a density corresponding to 10m visibility. For the ROADVIEW tests, we chose to focus on fogs with MORs of 10m, 20m, 30m and 50m. Indeed, these fogs are identified as relevant because it is in this range that most sensors (camera, lidar) have detection problems [14] [15] [16].

The PAVIN platform is capable of stabilizing fogs for test purposes [3]. However, there is always an error, as this stabilization process is complicated. For this reason, it is important to qualify more precisely the fogs present during each test. Figure 27 shows the recorded MOR as a function of the desired MOR for all tests. The figure shows that the measured MOR correlates very well with the target MOR. The correlation coefficient is 0.97. For some tests, there is a discrepancy between the target MOR and the measured MOR, particularly for a MOR of 50m. The PAVIN platform announces a tolerated deviation on MOR of plus or minus 15% from 20m and plus or minus 3m below 20m. Only 5 of the 89 tests carried out did not comply with this requirement. Appendix F gives the exact MOR during each trial, so that the models can be readjusted to the exact visibility if necessary.

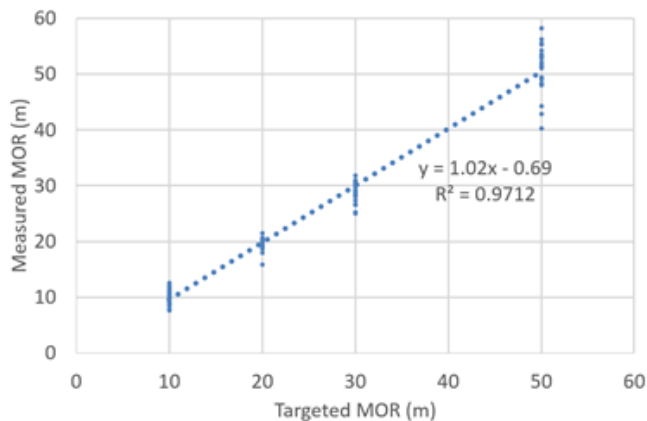


Figure 27 MOR measured as a function of target MOR during all tests (89 fog tests in total)

3.2.2 Microscopic fog validation: DSD

For the ROADVIEW tests, it was decided to use the small-drop fog proposed in the PAVIN platform [8]. A particle size measurement was nevertheless carried out, as the aim was to be able to feed the physical noise models with approximate laws. Figure 28 shows the average DSDs recorded for each visibility level. DSD measurement takes several minutes. As the tests carried out are too short, it was decided to propose an average DSD per visibility level, with the total quantity of droplets recalibrated to the visibility criterion. The DSDs obtained are in line with the usual DSDs of the platform, considering that the measurement was carried out over the radius range 0.3 - 20 microns [17].

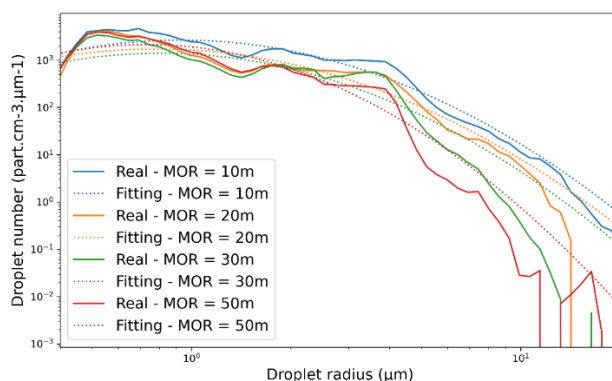


Figure 28 Fog Droplet Size Distributions during ROADVIEW testing

Physic-based models require simple DSD laws as input. Using a law allows us to characterize the DSD with just a few coefficients obtained by optimization on measured DSDs. Among other things, this eliminates the need for look-up tables in the noise models implemented, and therefore saves computing time. An optimization method was therefore implemented on the measured DSDs to obtain the coefficients of a log normal distribution [18]. Figure 28 shows the distributions obtained by fitting for each of the DSDs (dotted lines). The log normal distribution provides a good representation of the recorded data.

Table 11 summarizes the law coefficients obtained for the four fog densities selected, using the notations from [18].

MOR (m)	$\ln(\tilde{r})$	σ	N
10	0.484235252	0.74651233	6108.486
20	0.362382125	0.777099786	3559.641
30	0.334042672	0.742155699	2754.154
50	0.118386081	0.656240841	3189.711

Table 11 Log-normal coefficients obtained using the method in [18].

3.3 Data Visualization

This section is specifically tailored to demonstrate how the data inside the dataset looks like. It is divided into two parts, the data collected in controlled environments and the data collected in the Puy-de-Dome.

3.3.1 Data collected in controlled environments

Figure 29 specifically shows the point clouds observed during the test scenario rain.

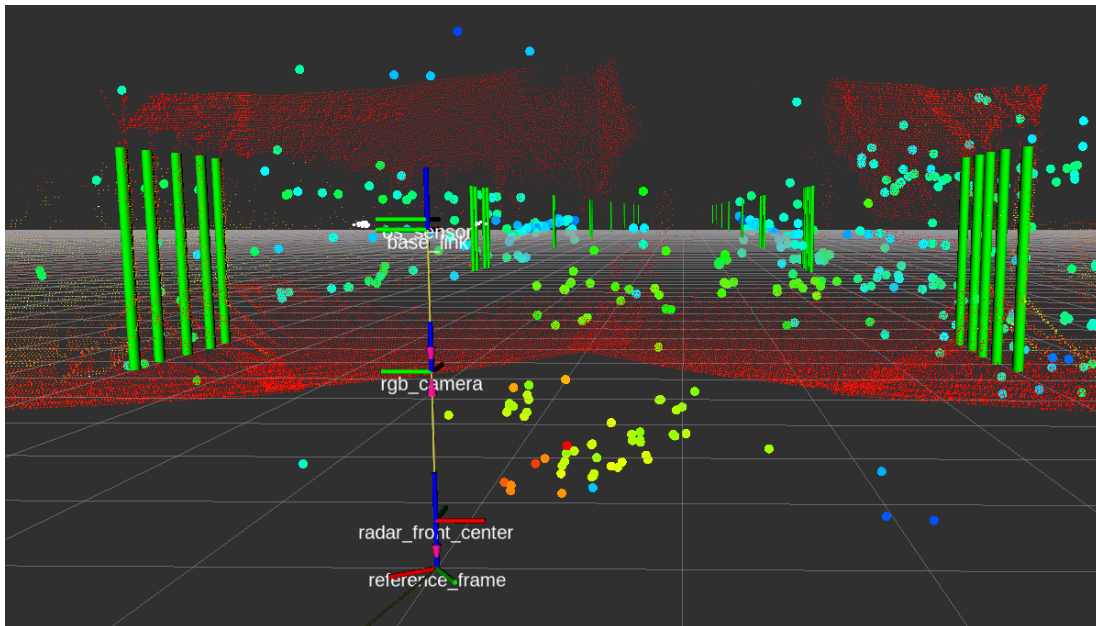


Figure 29 Point cloud visualization

Figure 29 shows the point clouds. The Innoviz One point cloud is represented in red, and the larger circular points are from the ZF ProWave RADAR. RTK positioned locations of the sprinklers are also represented in the figure as green vertical bars.



Figure 30 Dataset collected thermal camera image.

Figure 30 shows the thermal camera image that was collected in this specific frame, and Figure 31 show the captured image from the RGB camera.



Figure 31 Dataset collected RGB camera image.

3.3.2 Data collected with snow in Puy de DOME

During Puy-de-Dôme data collection, a total of 86 measurements with snow were collected. Including 1 minute of RADAR and LiDAR, 1 camera snapshot, and rainfall rates, temperature and fog MOR. The data can be seen in Table 12, where it can be seen different weather effect occurring : top left, snowflakes with wind and long exposure time (night conditions); top right, snowflakes without wind and short exposure time (day conditions); bottom left, snow on the ground which is changing surface properties (reflectivity); bottom right, snow on the camera lens. In the presence of snow, there is often also the presence of ambient fog, which is part of the noise to be modeled as part of tasks 3.3 and 3.4.

Table 12 Images from the Puy de Dome data collection

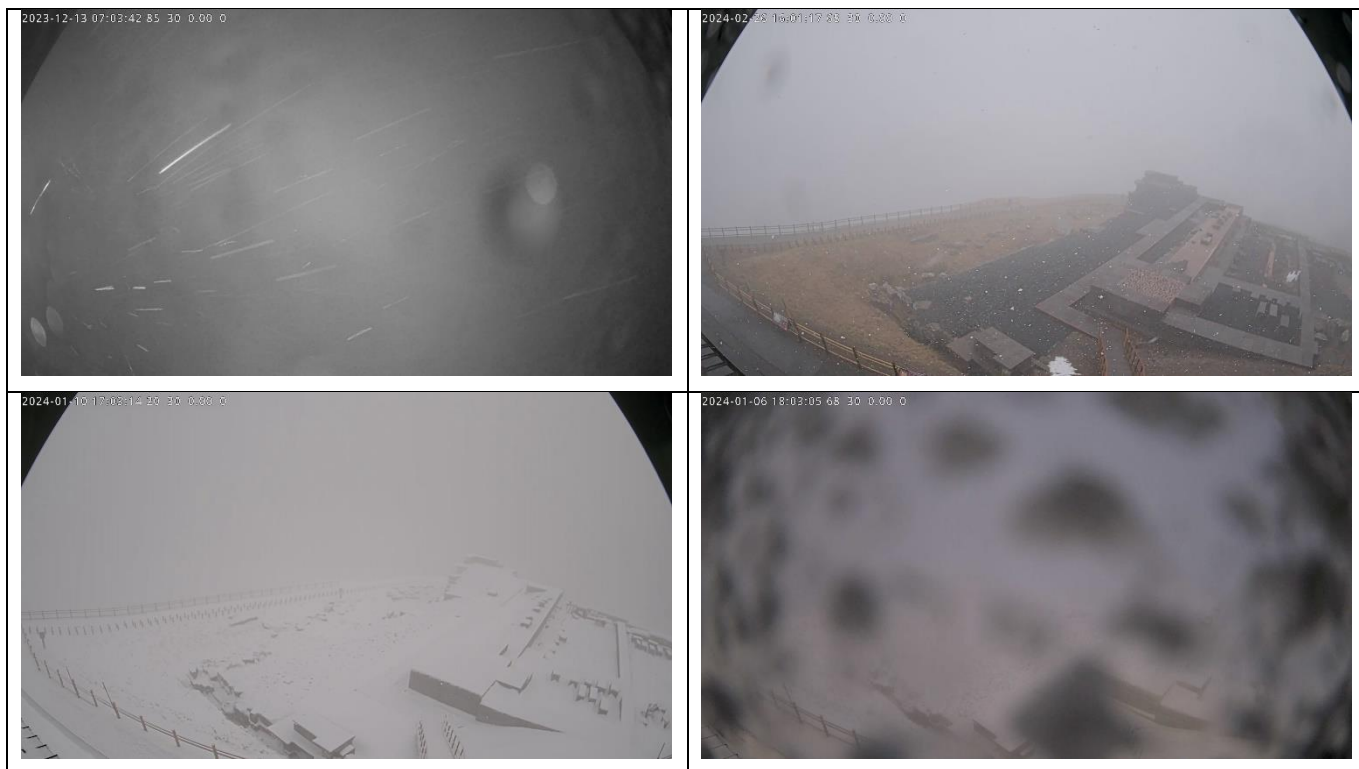


Figure 32 shows the Puy de Dome data collected from the LiDAR with snow. It is possible to see in the red circle the snowflakes in this specific collection.



Figure 32 Lidar point cloud with snow

3.4 Dataset Availability

The dataset weighs a total of 292.1GB and is divided into scenes between 41 GB and 48 GB.

The dataset was named REHEARSE due to it being specifically designed with the purpose of training and “rehearsing” noise sensor models. REHEARSE also happens to be an acronym for “adveRse wEatHEr datAsEt for sensoRy noiSe modElS”.


[REHEARSE Dataset](#) [Test Sites](#) [Sensor Setup](#) [Adverse Weather](#) [Download](#) [Contributors](#) [ROADVIEW Project](#)

REHEARSE: adveRse wEatHEr datAsEt for sensoRy noiSe modElS

Simulation has become an important part of automated vehicle development, but to have an accurate simulation, it is necessary to have correct and accurate sensor models, with this in mind in this project a dataset is created.

The project ROADVIEW uses the V Methodology to implement its algorithms, this implies that to develop and validate algorithms in this project it is required to do simulation. For a simulation to be close to its reality counterpart, the proposed methodology is to use XIL (everything in the loop), but for the XIL environment to close the simulation-to-reality gap, one of the requirements is to have the sensor’s noise model. The importance of closing the simulation-to-reality gap is noted by authorities also such as seen in [1], where the German Ministry has underlined the importance of testing algorithms using simulation and that the simulation-to-reality gap must be small. An example of a technic to lower this gap is seen in [2] where a camera is seen in the simulation loop. Simulation provides the ability to propose safety critical scenarios, and quick down time to change scenarios.

The ROADVIEW project tackles this requirement of a low simulation-to-reality gap in many ways, one of them is by generating sensor noise models. The creation of this noise models requires a dataset with data from the sensors that will be utilized in the XIL environment. As the goal of ROADVIEW is to create a robust adverse weather algorithm, the models must be created to adverse weather conditions. Therefore, this work discusses creation of a dataset that will support the development of the further sensor models. The dataset requires different distances (from close to far), and different weather conditions (ranging from clear to harsh), in such case, the data collection for this work was made in the CARISSMA and CEREMA PAVIN proving Ground, as they have complementary abilities regarding synthetic rain generation, and CE has fog generation. As shown in the below Figure 1, CE (light blue in the figure) can produce more rain but at closer distances compared to CARISSMA (dark blue in the figure), where there is less rain but has a larger total size of the test track.



Funded by the European Union (grant no. 101069576). Views and opinions expressed are however those of the author(s) only and do not necessarily reflect those of the European Union or the European Climate, Infrastructure and Environment Executive Agency (CINEA). Neither the European Union nor the granting authority can be held responsible for them. UK and Swiss participants in this project are supported by Innovate UK (contract no. 10045139) and the Swiss State Secretariat for Education, Research and Innovation (Contract no.22.00123) respectively.

Figure 33 Landing Page REHEARSE Website Layout

A website [19] was developed to work as a landing page for those who might be interested in the dataset, as well as providing information on how the dataset was created. Figure 33 shows how the website is currently formatted, and available for the public.

4 Conclusion

The V methodology used in the ROADVIEW project requires the development of sensor models for further usage in the XIL environment. These sensors models will work together with other WP to lower the simulation-to-reality gap. To produce these sensor models a dataset with the sensor information is required. This work discusses the methodology behind the production such a dataset in two distinct test facilities: one in CE and one in THI. A 291 GB dataset is produced and made available at [19] (RISE repository).

This dataset is obtained through recordings using different sensors with different capabilities and sensing methodologies in the THI and CE proving grounds. The usage of complementary proving grounds provides substantial ampliation of the test suite to include from outdoor scenarios to indoor fog. This report describes the methodology regarding how this data was recorded, stored and postprocessed. The fidelity of the synthetic rain produced in each of the test places is also validated. Indications regarding the location and reflectivity values of different targets are included in the dataset.

This dataset counts with 151 total scenes with:

- 92 clean rain scenarios,
- 37 pedestrian scenarios,
- 43 bicycle scenarios,
- 28 target scenarios,
- 103-day scenarios,
- 48-night scenarios,
- 60 clear weather scenarios,
- 91 rain scenarios, and
- 86 cases of snow at the Puy de Dome.

In this dataset the rain scenarios, the rain was validated using disdrometers and a weather station. In the THI outdoor scenarios with rain, it was demonstrated that the rain moves as expected with the wind, but the rain DSD is uniformly distributed in the region of interest. The outdoor test track also proved to have less RADAR reflections than the indoor test track. The THI outdoor test track has a longer maximum distance with a total of a continuous rain for 118m at 10mm/h.

The CE test track proved to have a very important impact on the dataset, with it delivering a substantially higher amount of rain (165mm/h) than the THI outdoor (50mm/h) but at smaller distances (maximum 28m). The behaviour of the rain was also measured and found that due to the construction of the proving ground, the rain rates were smaller than expected to higher rain rates. The CE test track also brought to the table fog generation to the dataset.

Different scenarios were separated into different folders and are made publicly available in an OSI format, allowing to substantially reduce its size compared to the original rosbag size, as well as being a ASAM standard for simulation, increasing the strength of the published dataset.

This work feeds forward to WP3, WP5, and WP6, being an important part of developing the sensor models and the denoising algorithms. Point cloud labelling is an important part of the work that allows increases the use of this dataset from only sensor model creation and expands it to multiple other uses, such as machine learning. For this, the partner involved in this work will collaborate with other tasks which will help with point cloud labelling, to further improve the dataset quality towards the development of algorithms.

References

- [1] Bundesministerium für digitales und verkehr, "Bundesministeriums für digitales und verkehr 86/22," Bundesministerium für digitales und verkehr, 2022.
- [2] F. Reway, A. Hoffmann, D. Wachtel, W. Huber, A. Knoll and E. Ribeiro, "Test Method for Measuring the Simulation-to-Reality Gap of Camera-based Object Detection Algorithms for Autonomous Driving," 2020 IEEE Intelligent Vehicles Symposium (IV), p. 1249–1256, 2020.
- [3] S. Liandrat, P. Duthon, F. Bernardin, A. B. Daoued and J.-L. Bicard, "A review of Cerema PAVIN fog & rain platform: from past and back to the future," in ITS World Congress, Los Angeles, Chicago, 2022.
- [4] M. Colomb, P. Duthon and S. Laukkanen, "Deliverable D 2.1 : Characteristics of Adverse Weather Conditions," 2017.
- [5] World Meteorological Organization (WMO), The Guide to Hydrological Practices (WMO No.168), vol. 2, World Meteorological Organization, 2009, pp. II.5-1 - II.5-60.
- [6] L. C. D. Silva, M. F. Drechsler, Y. Poledna, W. Huber and T. Antonio Fiorentin, "Synthetic Extreme Weather for AI Training: Concept and Validation," in 2023 Third International Conference on Digital Data Processing (DDP), Luton, 2023.
- [7] W. Na and C. Yoo, "Evaluation of rainfall temporal distribution models with annual maximum rainfall events in Seoul, Korea," MDPI, vol. 10, no. 10, p. 1468, 2018.
- [8] P. Duthon, M. Colomb and F. Bernardin, "Fog classification by their droplet size distributions. Application to the characterization of Cerema's PAVIN BP plateform (under review)," Atmosphere, 2020.
- [9] S. A. I. L. e. al., "Robotic Operating System," [Online]. Available: <https://www.ros.org>. [Accessed 27 10 2023].
- [10] T. Hanke, N. Hirsenkorn, C. van-Driesten, P. Garcia-Ramos, M. Schiementz, S. Schneider and E. Biebl, "A generic interface for the environment perception of automated driving functions in virtual scenarios.," 2017.
- [11] T. Laurila, V. Sinclair and H. Gregow, "Climatology, variability and trends in near-surface wind speeds over the North Atlantic and Europe during 1979–2018 based on ERA5," International Journal of Climatology, vol. 41, 2020.
- [12] L. Johannsen, N. Zambon, P. Strauss, T. Dostal, M. Neumann, D. Zumr, T. Cochrane, G. Blöschl and A. Klik, "Comparison of three types of laser optical disdrometers under natural rainfall conditions.," Hydrol Sci J., vol. 65, no. 4, pp. 524-535, 2020.
- [13] J. S. Marshall and W. M. Palmer, "The distribution of raindrops with size," J. Meteor., vol. 5, pp. 165-166, 1948.
- [14] M. Bijelic, T. Gruber and W. Ritter, "A Benchmark for Lidar Sensors in Fog: Is Detection Breaking Down?," IEEE Intelligent Vehicles Symposium, Proceedings, Vols. 2018-June, no. Iv, pp. 760-767, 2018.
- [15] Y. Li, P. Duthon, M. Colomb and J. Ibanez-Guzman, "What happens for a ToF LiDAR in fog?," Transactions on Intelligent Transportation Systems, 2020.
- [16] K. Montalban, C. Reymann, D. Atchuthan, P.-E. Dupouy, N. Riviere and S. Lacroix, "A Quantitative Analysis of Point Clouds from Automotive Lidars Exposed to Artificial Rain and Fog," Atmosphere, vol. 12, 2021.
- [17] P. Duthon, M. Colomb and F. Bernardin, "Light Transmission in Fog: The Influence of Wavelength on the Extinction Coefficient," Applied Sciences, vol. 9, no. 14, p. 2843, 2019.
- [18] F. Bernardin, M. Colomb, F. Egal, P. Morange and J. Boreux, "Droplet distribution models for visibility calculation," 2010.

- [19] ROADVIEW CONSORTIUM, “Rehearse Dataset,” Technische Hochschule Ingolstadt and RISE AG, 14 11 2023. [Online]. Available: <https://s3.ice.ri.se/roadview-WP3-Warwick/T3.2%20-%20Create%20Dataset/rehearse/index.html>. [Accessed 14 11 2023].
- [20] J. Rivera, L. Khoudour, G. Saint Pierre, P. Duthon, S. Liandrat, F. Bernardin, S. Fiss, I. Ivanov and R. Peleg, “Analysis of Thermal Imaging Performance under Extreme Foggy Conditions: Applications to Autonomous Driving,” *Journal of Imaging*, vol. 8, p. 306, 2022.
- [21] W. M. Organization, *Guide to Meteorological Instruments and Methods of Observation* (2014 edition updated in 2017; WMO-No. 8), World Meteorological Organization, 2014, p. 1163.
- [22] L. Sébastien, D. Pierre, B. Frédéric and B. D. Amine, “A review of Cerema PAVIN fog & rain platform: from past and back to the future,” in », ITS World Congress, Los, 2022.

Appendix A. Actor position in the THI proving ground using RTK coordinates.

Table 13 Sprinkler location in RTK coordinates and sensor referenced locations.

Mounting positions				
Object	Sensor relative position		Locally based RTK	
	X (m)	Y (m)	Latitude (m)	Longitude (m)
Sensor	0	0	-32,45	-35,62
Sprinkler 1	5,5	4	-38,82	-38,08
Sprinkler 2	5,5	-4	-32,05	-42,42
Sprinkler 3	6	4	-39,05	-38,53
Sprinkler 4	6	-4	-32,31	-42,85
Sprinkler 5	6,5	4	-39,3	-38,93
Sprinkler 6	6,5	-4	-32,62	-43,28
Sprinkler 7	7	4	-39,59	-39,33
Sprinkler 8	7	-4	-32,9	-43,65
Sprinkler 9	7,5	4	-39,87	-39,77
Sprinkler 10	7,5	-4	-33,13	-44,12
Sprinkler 11	21,5	4	-47,44	-51,52
Sprinkler 12	21,5	-4	-40,73	-55,86
Sprinkler 13	22	4	-47,72	-51,94
Sprinkler 14	22	-4	-41	-56,3
Sprinkler 15	22,5	4	-48	-52,38
Sprinkler 16	22,5	-4	-41,28	-46,73
Sprinkler 17	23	4	-48,28	-52,8
Sprinkler 18	23	-4	-41,56	-57,15
Sprinkler 19	23,5	4	-48,56	-53,19
Sprinkler 20	23,5	-4	-41,82	-57,54
Sprinkler 21	37,5	4	-56,14	-64,94
Sprinkler 22	37,5	-4	-49,4	-69,3
Sprinkler 23	53,5	4	-64,81	-78,4

Mounting positions				
Object	Sensor relative position		Locally based RTK	
	X (m)	Y (m)	Latitude (m)	Longitude (m)
Sprinkler 24	53,5	-4	-58,08	-82,77
Sprinkler 25	38	4	-56,42	-65,38
Sprinkler 26	38	-4	-49,65	-69,75
Sprinkler 27	54	4	-65,09	-78,82
Sprinkler 28	54	-4	-58,35	-83,18
Sprinkler 29	38,5	4	-56,58	-65,78
Sprinkler 30	54,5	-4	-58,62	-83,58
Sprinkler 31	69,5	4	-73,4	-91,87
Sprinkler 32	69,5	-4	-66,79	-96,21
Sprinkler 33	85,5	4	-82,14	-105,3
Sprinkler 34	85,5	-4	-75,45	-109,66
Sprinkler 35	101,5	4	-90,73	-118,68
Sprinkler 36	101,5	-4	-84,17	-123,07
Sprinkler 37	117,5	4	-99,53	-132,17
Sprinkler 38	117,5	-4	-92,43	-136,33
Target 1	28	0	-47,62	-59,17
Target 2	56	0	-62,82	-82,74
Target 3	84	0	-77,9	-106,15
Target 4	112	0	-93,18	-129,74

Note: Sprinkler 16 does not have the exact RTK coordinates due to it being an inconsistent location, therefore as the data was wrong it was removed.

Appendix B. THI CARISSMA Test Suite

Table 14 CARISSMA test suit

Test	Description	Sprinkler position	Target	Distance (m)	Angle	Time	
1.1	Dry day	Position 1	Pedestrian	28	0°	10	
1.2				28	45°	2	
1.3				28	90°	2	
1.4				56	0°	2	
1.5				56	45°	2	
1.6				56	90°	2	
1.7				84	0°	2	
1.8				84	45°	2	
1.9				84	90°	2	
1.10				112	0°	2	
1.11				112	45°	2	
1.12				112	90°	2	
1.13			Bicycle	28	0°	10	
1.14				28	45°	2	
1.15				28	90°	2	
1.16				56	0°	2	
1.17				56	45°	2	
1.18				56	90°	2	
1.19				84	0°	2	
1.20				84	45°	2	
1.21				84	90°	2	
1.22				112	0°	2	
1.23				112	45°	2	
1.24				112	90°	2	
1.25				Car	28	0°	10
1.26					28	45°	2
1.27					28	90°	2

Test	Description	Sprinkler position	Target	Distance (m)	Angle	Time	
1.28				56	0°	2	
1.29	Dry day	Position 1	Car	56	45°	2	
1.30				56	90°	2	
1.31				84	0°	2	
1.32				84	45°	2	
1.33				84	90°	2	
1.34				112	0°	2	
1.35				112	45°	2	
1.36				112	90°	2	
1.37				Corner reflector	112	0°	10
1.38					56	0°	2
1.39			84		0°	2	
1.40			112		0°	2	
1.41			LiDAR targets	28	0°	10	
1.42				56	0°	2	
1.43				84	0°	2	
1.44				112	0°	2	
1.41			Camera targets	28	0°	10	
1.42				56	0°	2	
1.43				84	0°	2	
1.44				112	0°	2	
2.1	Dry night	Position 1	Pedestrian	28	0°	10	
2.2				56	0°	2	
2.3				84	0°	2	
2.4				112	0°	2	
2.5			Bicycle	28	0°	10	
2.6				56	0°	2	
2.7				84	0°	2	
2.8				112	0°	2	

Test	Description	Sprinkler position	Target	Distance (m)	Angle	Time
2.9			Car	28	0°	10
2.10	Dry night	Position 1	Car	56	0°	2
2.11				84	0°	2
2.12				112	0°	2
2.13			Corner reflector	28	0°	10
2.14				56	0°	2
2.15				84	0°	2
2.16				112	0°	2
2.17			LiDAR targets	28	0°	10
2.18				56	0°	2
2.19				84	0°	2
2.20				112	0°	2
2.21			Camera targets	28	0°	10
2.22				56	0°	2
2.23				84	0°	2
2.24				112	0°	2
3.1			Dry day	Position 1	Pedestrian	28
3.2	28	45°				2
3.3	28	90°				2
3.4	56	0°				2
3.5	56	45°				2
3.6	56	90°				2
3.7	84	0°				2
3.8	84	45°				2
3.9	84	90°				2
3.10	112	0°				2
3.11	112	45°				2
3.12	112	90°				2
3.13					Bicycle	28

Test	Description	Sprinkler position	Target	Distance (m)	Angle	Time	
3.14				28	45°	2	
3.15	Dry day	Position 1	Bicycle	28	90°	2	
3.16				56	0°	2	
3.17				56	45°	2	
3.18				56	90°	2	
3.19				84	0°	2	
3.20				84	45°	2	
3.21				84	90°	2	
3.22				112	0°	2	
3.23				112	45°	2	
3.24				112	90°	2	
3.25				Car	28	0°	10
3.26					28	45°	2
3.27			28		90°	2	
3.28			56		0°	2	
3.29			56		45°	2	
3.30			56		90°	2	
3.31			84		0°	2	
3.32			84		45°	2	
3.33			84		90°	2	
3.34			112		0°	2	
3.35			112		45°	2	
3.36			112		90°	2	
3.37			Corner reflector	112	0°	10	
3.38				56	0°	2	
3.39				84	0°	2	
3.40				112	0°	2	
3.41			LiDAR targets	28	0°	10	
3.42				56	0°	2	

Test	Description	Sprinkler position	Target	Distance (m)	Angle	Time
3.43				84	0°	2
3.44	Dry day	Position 1	LIDAR targets	112	0°	2
3.45			Camera targets	28	0°	10
3.46				56	0°	2
3.47				84	0°	2
3.48				112	0°	2
4.1	Dry night	Position 1	Pedestrian	28	0°	10
4.2				56	0°	2
4.3				84	0°	2
4.4				112	0°	2
4.5			Bicycle	28	0°	10
4.6				56	0°	2
4.7				84	0°	2
4.8				112	0°	2
4.9			Car	28	0°	10
4.10				56	0°	2
4.11				84	0°	2
4.12				112	0°	2
4.13			Corner reflector	28	0°	10
4.14				56	0°	2
4.15				84	0°	2
4.16				112	0°	2
4.17			LiDAR targets	28	0°	10
4.18				56	0°	2
4.19				84	0°	2
4.20				112	0°	2
4.21	Camera targets	28	0°	10		
4.22		56	0°	2		
4.23		84	0°	2		

Test	Description	Sprinkler position	Target	Distance (m)	Angle	Time
4.24				112	0°	2
5.1	25 mm/h night	Position 2	Pedestrian	28	0°	10
5.2				28	45°	2
5.3				28	90°	2
5.4				56	0°	2
5.5				56	45°	2
5.6				56	90°	2
5.7				Bicycle	28	0°
5.8			28		45°	2
5.9			28		90°	2
5.10			56		0°	2
5.11			56		45°	2
5.12			56		90°	2
5.13			Car	28	0°	10
5.14				28	45°	2
5.15				28	90°	2
5.16				56	0°	2
5.17				56	45°	2
5.18				56	90°	2
5.19			Corner reflector	28	0°	10
5.20				56	0°	2
5.21			LiDAR targets	28	0°	10
5.22				56	0°	2
5.23			Camera targets	28	0°	10
5.24				56	0°	2
6.1	25 mm/h night	Position 2	Pedestrian	28	0°	10
6.2				56	0°	2
6.3			Bicycle	28	0°	10
6.4				56	0°	2

Test	Description	Sprinkler position	Target	Distance (m)	Angle	Time
6.5			Car	28	0°	10
6.6	25 mm/h night	Position 2	Car	56	0°	2
6.7			Corner reflector	28	0°	10
6.8				56	0°	2
6.9			LiDAR targets	28	0°	10
6.10				56	0°	2
6.11			Camera targets	28	0°	10
6.12				56	0°	2
7.1			50 mm/h night	Position 3	Pedestrian	28
7.2	28	45°				2
7.3	28	90°				2
7.4	Bicycle	28			0°	10
7.5		28			45°	2
7.6		28			90°	2
7.7	Car	28			0°	10
7.8		28			45°	2
7.9		28			90°	2
7.10	Corner reflector	28			0°	10
7.11	LiDAR targets	28			0°	10
7.12	Camera targets	28			0°	10

Appendix C. CE test suite

Table 15 CE test suit

Test	Target	Ambient light condition / Ego vehicle headlight	Meteorological condition	Object surface state	Side wall lighting status	Distance sensor/targets
1	Calibrated	Day / Off	Fog @10m	Wet	Off	15m in Greenhouse
2	Calibrated	Day / Off	Fog @20m	Wet	Off	15m in Greenhouse
3	Calibrated	Day / Off	Fog @30m	Wet	Off	15m in Greenhouse
4	Calibrated	Day / Off	Fog @50m	Wet	Off	15m in Greenhouse
5	Calibrated	Day / Off	Rain @17mm/h	Wet	Off	15m in Greenhouse
6	Calibrated	Day / Off	Rain @50mm/h	Wet	Off	15m in Greenhouse
7	Calibrated	Day / Off	Rain @101mm/h	Wet	Off	15m in Greenhouse
8	Calibrated	Day / Off	Rain @175mm/h	Wet	Off	15m in Greenhouse
9	Calibrated	Night / On	Clear	Dry	Off	10m
10	Calibrated	Night / On	Clear	Dry	Off	19m
11	Calibrated	Night / On	Clear	Dry	Off	28m
12	Calibrated	Night / On	Clear	Dry	On	10m
13	Calibrated	Night / On	Clear	Dry	On	19m
14	Calibrated	Night / On	Clear	Dry	On	28m
15	Calibrated	Night / On	Clear	Wet	Off	10m
16	Calibrated	Night / On	Clear	Wet	Off	19m
17	Calibrated	Night / On	Clear	Wet	Off	28m

Co-funded by the European Union. Views and opinions expressed are however those of the author(s) only and do not necessarily reflect those of the European Union or European Climate, Infrastructure and Environment Executive Agency (CINEA). Neither the European Union nor the granting authority can be held responsible for them. Project grant no. 101069576.



UK participants in this project are co-funded by Innovate UK under contract no.10045139.
Swiss participants in this project are co-funded by the Swiss State Secretariat for Education, Research and Innovation (SERI) under contract no. 22.00123.

Test	Target	Ambient light condition / Ego vehicle headlight	Meteorological condition	Object surface state	Side wall lighting status	Distance sensor/targets
18	Calibrated	Night / On	Clear	Wet	On	10m
19	Calibrated	Night / On	Clear	Wet	On	19m
20	Calibrated	Night / On	Clear	Wet	On	28m
21	Calibrated	Night / On	Fog @10m	Wet	Off	10m
22	Calibrated	Night / On	Fog @10m	Wet	Off	19m
23	Calibrated	Night / On	Fog @10m	Wet	Off	28m
24	Calibrated	Night / On	Fog @10m	Wet	On	10m
25	Calibrated	Night / On	Fog @10m	Wet	On	19m
26	Calibrated	Night / On	Fog @10m	Wet	On	28m
27	Calibrated	Night / On	Fog @20m	Wet	Off	10m
28	Calibrated	Night / On	Fog @20m	Wet	Off	19m
29	Calibrated	Night / On	Fog @20m	Wet	Off	28m
30	Calibrated	Night / On	Fog @20m	Wet	On	10m
31	Calibrated	Night / On	Fog @20m	Wet	On	19m
32	Calibrated	Night / On	Fog @20m	Wet	On	28m
33	Calibrated	Night / On	Fog @30m	Wet	Off	10m
34	Calibrated	Night / On	Fog @30m	Wet	Off	19m
35	Calibrated	Night / On	Fog @30m	Wet	Off	28m

Test	Target	Ambient light condition / Ego vehicle headlight	Meteorological condition	Object surface state	Side wall lighting status	Distance sensor/targets
36	Calibrated	Night / On	Fog @30m	Wet	On	10m
37	Calibrated	Night / On	Fog @30m	Wet	On	19m
38	Calibrated	Night / On	Fog @30m	Wet	On	28m
39	Calibrated	Night / On	Fog @50m	Wet	Off	10m
40	Calibrated	Night / On	Fog @50m	Wet	Off	19m
41	Calibrated	Night / On	Fog @50m	Wet	Off	28m
42	Calibrated	Night / On	Fog @50m	Wet	On	10m
43	Calibrated	Night / On	Fog @50m	Wet	On	19m
44	Calibrated	Night / On	Fog @50m	Wet	On	28m
45	Calibrated	Night / On	Rain @17mm/h	Wet	Off	10m
46	Calibrated	Night / On	Rain @17mm/h	Wet	Off	19m
47	Calibrated	Night / On	Rain @17mm/h	Wet	Off	28m
48	Calibrated	Night / On	Rain @17mm/h	Wet	Off	28m
49	Calibrated	Night / On	Rain @17mm/h	Wet	On	10m
50	Calibrated	Night / On	Rain @17mm/h	Wet	On	19m
51	Calibrated	Night / On	Rain @17mm/h	Wet	On	28m
52	Calibrated	Night / On	Rain @17mm/h	Wet	On	28m
53	Calibrated	Night / On	Rain @50mm/h	Wet	Off	10m

Test	Target	Ambient light condition / Ego vehicle headlight	Meteorological condition	Object surface state	Side wall lighting status	Distance sensor/targets
54	Calibrated	Night / On	Rain @50mm/h	Wet	Off	19m
55	Calibrated	Night / On	Rain @50mm/h	Wet	Off	28m
56	Calibrated	Night / On	Rain @50mm/h	Wet	Off	28m
57	Calibrated	Night / On	Rain @50mm/h	Wet	On	10m
58	Calibrated	Night / On	Rain @50mm/h	Wet	On	19m
59	Calibrated	Night / On	Rain @50mm/h	Wet	On	28m
60	Calibrated	Night / On	Rain @50mm/h	Wet	On	28m
61	Calibrated	Night / On	Rain @101mm/h	Wet	Off	10m
62	Calibrated	Night / On	Rain @101mm/h	Wet	Off	19m
63	Calibrated	Night / On	Rain @101mm/h	Wet	Off	28m
64	Calibrated	Night / On	Rain @101mm/h	Wet	Off	28m
65	Calibrated	Night / On	Rain @101mm/h	Wet	On	10m
66	Calibrated	Night / On	Rain @101mm/h	Wet	On	19m
67	Calibrated	Night / On	Rain @101mm/h	Wet	On	28m
68	Calibrated	Night / On	Rain @101mm/h	Wet	On	28m
69	Calibrated	Night / On	Rain @175mm/h	Wet	Off	10m
70	Calibrated	Night / On	Rain @175mm/h	Wet	Off	19m
71	Calibrated	Night / On	Rain @175mm/h	Wet	Off	28m

Test	Target	Ambient light condition / Ego vehicle headlight	Meteorological condition	Object surface state	Side wall lighting status	Distance sensor/targets
72	Calibrated	Night / On	Rain @175mm/h	Wet	Off	28m
73	Calibrated	Night / On	Rain @175mm/h	Wet	On	10m
74	Calibrated	Night / On	Rain @175mm/h	Wet	On	19m
75	Calibrated	Night / On	Rain @175mm/h	Wet	On	28m
76	Calibrated	Night / On	Rain @175mm/h	Wet	On	28m
77	Car	Day / Off	Fog @10m	Wet	Off	15m in Greenhouse
78	Car	Day / Off	Fog @20m	Wet	Off	15m in Greenhouse
79	Car	Day / Off	Fog @30m	Wet	Off	15m in Greenhouse
80	Car	Day / Off	Fog @50m	Wet	Off	15m in Greenhouse
81	Car	Day / Off	Rain @17mm/h	Wet	Off	15m in Greenhouse
82	Car	Day / Off	Rain @50mm/h	Wet	Off	15m in Greenhouse
83	Car	Day / Off	Rain @101mm/h	Wet	Off	15m in Greenhouse
84	Car	Day / Off	Rain @175mm/h	Wet	Off	15m in Greenhouse
85	Car	Night / On	Clear	Dry	Off	10m
86	Car	Night / On	Clear	Dry	Off	19m
87	Car	Night / On	Clear	Dry	Off	28m
88	Car	Night / On	Clear	Dry	On	10m
89	Car	Night / On	Clear	Dry	On	19m

Test	Target	Ambient light condition / Ego vehicle headlight	Meteorological condition	Object surface state	Side wall lighting status	Distance sensor/targets
90	Car	Night / On	Clear	Dry	On	28m
91	Car	Night / On	Clear	Wet	Off	10m
92	Car	Night / On	Clear	Wet	Off	19m
93	Car	Night / On	Clear	Wet	Off	28m
94	Car	Night / On	Clear	Wet	On	10m
95	Car	Night / On	Clear	Wet	On	19m
96	Car	Night / On	Clear	Wet	On	28m
97	Car	Night / On	Fog @10m	Wet	Off	10m
98	Car	Night / On	Fog @10m	Wet	Off	19m
99	Car	Night / On	Fog @10m	Wet	Off	28m
100	Car	Night / On	Fog @10m	Wet	On	10m
101	Car	Night / On	Fog @10m	Wet	On	10m
102	Car	Night / On	Fog @10m	Wet	On	19m
103	Car	Night / On	Fog @10m	Wet	On	28m
104	Car	Night / On	Fog @20m	Wet	Off	10m
105	Car	Night / On	Fog @20m	Wet	Off	19m
106	Car	Night / On	Fog @20m	Wet	Off	28m
107	Car	Night / On	Fog @20m	Wet	On	10m

Test	Target	Ambient light condition / Ego vehicle headlight	Meteorological condition	Object surface state	Side wall lighting status	Distance sensor/targets
108	Car	Night / On	Fog @20m	Wet	On	10m
109	Car	Night / On	Fog @20m	Wet	On	19m
110	Car	Night / On	Fog @20m	Wet	On	28m
111	Car	Night / On	Fog @30m	Wet	Off	10m
112	Car	Night / On	Fog @30m	Wet	Off	19m
113	Car	Night / On	Fog @30m	Wet	Off	28m
114	Car	Night / On	Fog @30m	Wet	On	10m
115	Car	Night / On	Fog @30m	Wet	On	10m
116	Car	Night / On	Fog @30m	Wet	On	19m
117	Car	Night / On	Fog @30m	Wet	On	28m
118	Car	Night / On	Fog @50m	Wet	Off	10m
119	Car	Night / On	Fog @50m	Wet	Off	19m
120	Car	Night / On	Fog @50m	Wet	Off	28m
121	Car	Night / On	Fog @50m	Wet	On	10m
122	Car	Night / On	Fog @50m	Wet	On	10m
123	Car	Night / On	Fog @50m	Wet	On	19m
124	Car	Night / On	Fog @50m	Wet	On	28m
125	Car	Night / On	Rain @17mm/h	Wet	Off	10m

Test	Target	Ambient light condition / Ego vehicle headlight	Meteorological condition	Object surface state	Side wall lighting status	Distance sensor/targets
126	Car	Night / On	Rain @17mm/h	Wet	Off	19m
127	Car	Night / On	Rain @17mm/h	Wet	Off	28m
128	Car	Night / On	Rain @17mm/h	Wet	On	10m
129	Car	Night / On	Rain @17mm/h	Wet	On	19m
130	Car	Night / On	Rain @17mm/h	Wet	On	28m
131	Car	Night / On	Rain @17mm/h	Wet	On	15m in Greenhouse
132	Car	Night / On	Rain @50mm/h	Wet	Off	10m
133	Car	Night / On	Rain @50mm/h	Wet	Off	19m
134	Car	Night / On	Rain @50mm/h	Wet	Off	28m
135	Car	Night / On	Rain @50mm/h	Wet	On	10m
136	Car	Night / On	Rain @50mm/h	Wet	On	19m
137	Car	Night / On	Rain @50mm/h	Wet	On	28m
138	Car	Night / On	Rain @50mm/h	Wet	On	15m in Greenhouse
139	Car	Night / On	Rain @101mm/h	Wet	Off	10m
140	Car	Night / On	Rain @101mm/h	Wet	Off	19m
141	Car	Night / On	Rain @101mm/h	Wet	Off	28m
142	Car	Night / On	Rain @101mm/h	Wet	On	10m
143	Car	Night / On	Rain @101mm/h	Wet	On	19m

Test	Target	Ambient light condition / Ego vehicle headlight	Meteorological condition	Object surface state	Side wall lighting status	Distance sensor/targets
144	Car	Night / On	Rain @101mm/h	Wet	On	28m
145	Car	Night / On	Rain @101mm/h	Wet	On	15m in Greenhouse
146	Car	Night / On	Rain @175mm/h	Wet	Off	10m
147	Car	Night / On	Rain @175mm/h	Wet	Off	19m
148	Car	Night / On	Rain @175mm/h	Wet	Off	28m
149	Car	Night / On	Rain @175mm/h	Wet	On	10m
150	Car	Night / On	Rain @175mm/h	Wet	On	19m
151	Car	Night / On	Rain @175mm/h	Wet	On	28m
152	Car	Night / On	Rain @175mm/h	Wet	On	15m in Greenhouse
153	Ped.+Bike	Day / Off	Fog @10m	Wet	Off	15m in Greenhouse
154	Ped.+Bike	Day / Off	Fog @20m	Wet	Off	15m in Greenhouse
155	Ped.+Bike	Day / Off	Fog @30m	Wet	Off	15m in Greenhouse
156	Ped.+Bike	Day / Off	Fog @50m	Wet	Off	15m in Greenhouse
157	Ped.+Bike	Day / Off	Rain @17mm/h	Wet	Off	15m in Greenhouse
158	Ped.+Bike	Day / Off	Rain @50mm/h	Wet	Off	15m in Greenhouse
159	Ped.+Bike	Day / Off	Rain @101mm/h	Wet	Off	15m in Greenhouse
160	Ped.+Bike	Day / Off	Rain @175mm/h	Wet	Off	15m in Greenhouse
161	Ped.+Bike	Night / On	Clear	Dry	Off	10m

Test	Target	Ambient light condition / Ego vehicle headlight	Meteorological condition	Object surface state	Side wall lighting status	Distance sensor/targets
162	Ped.+Bike	Night / On	Clear	Dry	Off	19m
163	Ped.+Bike	Night / On	Clear	Dry	Off	28m
164	Ped.+Bike	Night / On	Clear	Dry	On	10m
165	Ped.+Bike	Night / On	Clear	Dry	On	19m
166	Ped.+Bike	Night / On	Clear	Dry	On	28m
167	Ped.+Bike	Night / On	Clear	Wet	Off	10m
168	Ped.+Bike	Night / On	Clear	Wet	Off	19m
169	Ped.+Bike	Night / On	Clear	Wet	Off	28m
170	Ped.+Bike	Night / On	Clear	Wet	On	10m
171	Ped.+Bike	Night / On	Clear	Wet	On	19m
172	Ped.+Bike	Night / On	Clear	Wet	On	28m
173	Ped.+Bike	Night / On	Fog @10m	Wet	Off	10m
174	Ped.+Bike	Night / On	Fog @10m	Wet	Off	19m
175	Ped.+Bike	Night / On	Fog @10m	Wet	Off	28m
176	Ped.+Bike	Night / On	Fog @10m	Wet	On	10m
177	Ped.+Bike	Night / On	Fog @10m	Wet	On	19m
178	Ped.+Bike	Night / On	Fog @10m	Wet	On	28m
179	Ped.+Bike	Night / On	Fog @20m	Wet	Off	10m

Test	Target	Ambient light condition / Ego vehicle headlight	Meteorological condition	Object surface state	Side wall lighting status	Distance sensor/targets
180	Ped.+Bike	Night / On	Fog @20m	Wet	Off	19m
181	Ped.+Bike	Night / On	Fog @20m	Wet	Off	28m
182	Ped.+Bike	Night / On	Fog @20m	Wet	On	10m
183	Ped.+Bike	Night / On	Fog @20m	Wet	On	19m
184	Ped.+Bike	Night / On	Fog @20m	Wet	On	28m
185	Ped.+Bike	Night / On	Fog @30m	Wet	Off	10m
186	Ped.+Bike	Night / On	Fog @30m	Wet	Off	19m
187	Ped.+Bike	Night / On	Fog @30m	Wet	Off	28m
188	Ped.+Bike	Night / On	Fog @30m	Wet	On	10m
189	Ped.+Bike	Night / On	Fog @30m	Wet	On	19m
190	Ped.+Bike	Night / On	Fog @30m	Wet	On	28m
191	Ped.+Bike	Night / On	Fog @50m	Wet	Off	10m
192	Ped.+Bike	Night / On	Fog @50m	Wet	Off	19m
193	Ped.+Bike	Night / On	Fog @50m	Wet	Off	28m
194	Ped.+Bike	Night / On	Fog @50m	Wet	On	10m
195	Ped.+Bike	Night / On	Fog @50m	Wet	On	19m
196	Ped.+Bike	Night / On	Fog @50m	Wet	On	28m
197	Ped.+Bike	Night / On	Rain @17mm/h	Wet	Off	10m

Test	Target	Ambient light condition / Ego vehicle headlight	Meteorological condition	Object surface state	Side wall lighting status	Distance sensor/targets
198	Ped.+Bike	Night / On	Rain @17mm/h	Wet	Off	19m
199	Ped.+Bike	Night / On	Rain @17mm/h	Wet	Off	28m
200	Ped.+Bike	Night / On	Rain @17mm/h	Wet	On	10m
201	Ped.+Bike	Night / On	Rain @17mm/h	Wet	On	19m
202	Ped.+Bike	Night / On	Rain @17mm/h	Wet	On	28m
203	Ped.+Bike	Night / On	Rain @50mm/h	Wet	Off	10m
204	Ped.+Bike	Night / On	Rain @50mm/h	Wet	Off	19m
205	Ped.+Bike	Night / On	Rain @50mm/h	Wet	Off	28m
206	Ped.+Bike	Night / On	Rain @50mm/h	Wet	On	10m
207	Ped.+Bike	Night / On	Rain @50mm/h	Wet	On	19m
208	Ped.+Bike	Night / On	Rain @50mm/h	Wet	On	28m
209	Ped.+Bike	Night / On	Rain @101mm/h	Wet	Off	10m
210	Ped.+Bike	Night / On	Rain @101mm/h	Wet	Off	19m
211	Ped.+Bike	Night / On	Rain @101mm/h	Wet	Off	28m
212	Ped.+Bike	Night / On	Rain @101mm/h	Wet	On	10m
213	Ped.+Bike	Night / On	Rain @101mm/h	Wet	On	19m
214	Ped.+Bike	Night / On	Rain @101mm/h	Wet	On	28m
215	Ped.+Bike	Night / On	Rain @175mm/h	Wet	Off	10m

Test	Target	Ambient light condition / Ego vehicle headlight	Meteorological condition	Object surface state	Side wall lighting status	Distance sensor/targets
216	Ped.+Bike	Night / On	Rain @175mm/h	Wet	Off	19m
217	Ped.+Bike	Night / On	Rain @175mm/h	Wet	Off	28m
218	Ped.+Bike	Night / On	Rain @175mm/h	Wet	On	10m
219	Ped.+Bike	Night / On	Rain @175mm/h	Wet	On	19m
220	Ped.+Bike	Night / On	Rain @175mm/h	Wet	On	28m

Appendix D. Disdrometer Location CE

Table 16 CE Disdrometer Location

Test	Clima Thies	Scale 1	OTT Parsivel	Scale 2	Scale 3	Scale 4
1	A1	A2	A3	D1	D2	D3
2	A1	A2	A3	D1	D2	D3
3	A1	A2	A3	D1	D2	D3
4	A1	A2	A3	D1	D2	D3
5	A2	A3	A1	D1	D2	D3
6	A2	A3	A1	D1	D2	D3
7	A2	A3	A1	D1	D2	D3
8	A2	A3	A1	D1	D2	D3
9	A3	A1	A2	D1	D2	D3
10	A3	A1	A2	D1	D2	D3
11	A3	A1	A2	D1	D2	D3
12	A3	A1	A2	D1	D2	D3
13	B1	B2	B3	C1	C2	C3
14	B1	B2	B3	C1	C2	C3
15	B1	B2	B3	C1	C2	C3
16	B1	B2	B3	C1	C2	C3
17	B2	B3	B1	C1	C2	C3
18	B2	B3	B1	C1	C2	C3
19	B2	B3	B1	C1	C2	C3
20	B2	B3	B1	C1	C2	C3
21	B3	B1	B2	C1	C2	C3
22	B3	B1	B2	C1	C2	C3
23	B3	B1	B2	C1	C2	C3
24	B3	B1	B2	C1	C2	C3
25	C1	C2	C3	B1	B2	B3
26	C1	C2	C3	B1	B2	B3
27	C1	C2	C3	B1	B2	B3
28	C1	C2	C3	B1	B2	B3
29	C2	C3	C1	B1	B2	B3
30	C2	C3	C1	B1	B2	B3
31	C2	C3	C1	B1	B2	B3
32	C2	C3	C1	B1	B2	B3
33	C3	C1	C2	B1	B2	B3



Co-funded by the European Union. Views and opinions expressed are however those of the author(s) only and do not necessarily reflect those of the European Union or European Climate, Infrastructure and Environment Executive Agency (CINEA). Neither the European Union nor the granting authority can be held responsible for them. Project grant no. 101069576.

UK participants in this project are co-funded by Innovate UK under contract no.10045139.
Swiss participants in this project are co-funded by the Swiss State Secretariat for Education, Research and Innovation (SERI) under contract no. 22.00123.

Test	Clima Thies	Scale 1	OTT Parsivel	Scale 2	Scale 3	Scale 4
34	C3	C1	C2	B1	B2	B3
35	C3	C1	C2	B1	B2	B3
36	C3	C1	C2	B1	B2	B3
37	D1	D2	D3	A1	A2	A3
38	D1	D2	D3	A1	A2	A3
39	D1	D2	D3	A1	A2	A3
40	D1	D2	D3	A1	A2	A3
41	D2	D3	D1	A1	A2	A3
42	D2	D3	D1	A1	A2	A3
43	D2	D3	D1	A1	A2	A3
44	D2	D3	D1	A1	A2	A3
45	D3	D1	D2	A1	A2	A3
46	D3	D1	D2	A1	A2	A3
47	D3	D1	D2	A1	A2	A3
48	D3	D1	D2	A1	A2	A3

Appendix E. Disdrometer Location THI

Table 17 THI Disdrometer Location

Mounting positions				
Rain measurement	Sensor relative position		Locally based RTK	
	X	Y	Latitude (m)	Longitude (m)
	(m)	(m)		
1	7	2	-37,93	-40,54
2	7	0	-36,26	-41,57
3	7	-2	-34,57	-42,61
4	14	2	-41,73	-46,34
5	14	0	-40,05	-47,42
6	14	-2	-38,35	-48,45
7	21	2	-45,56	-52,29
8	21	0	-43,83	-53,29
9	21	-2	-42,15	-54,35
10	28	2	-49,27	-58,13
11	28	0	-47,62	-59,17
12	28	-2	-46,05	-60,12
13	42	2	-56,9	-69,83
14	42	0	-55,21	-70,92
15	42	-2	-53,55	-71,97
16	56	2	-64,48	-81,58
17	56	0	-62,82	-82,74
18	56	-2	-61,07	-83,75
19	70	2	-72,05	-93,37
20	70	0	-70,54	-94,47
21	70	-2	-68,76	-95,72
22	84	2	-79,67	-105,13

Mounting positions				
Rain measurement	Sensor relative position		Locally based RTK	
	X	Y	Latitude (m)	Longitude (m)
	(m)	(m)		
23	84	0	-77,9	-106,15
24	84	-2	-76,3	-107,31
25	98	2	-87,2	-116,88
26	98	0	-85,55	-118,03
27	98	-2	-83,88	-119,16
28	112	2	-94,85	-128,66
29	112	0	-93,18	-129,74
30	112	-2	-91,54	-130,8

Appendix F. Measured Fog MOR for each test.

Target	Day/Night	Weather	Target MOR (m)	Lights	File	Start Time	Measured MOR (m)
01_ped_bike	01_night	03_fog	10	01_lights_on	10m.bag	06/06/2023 13:42	11
01_ped_bike	01_night	03_fog	10	01_lights_on	19m.bag	06/06/2023 13:44	9
01_ped_bike	01_night	03_fog	10	01_lights_on	28m.bag	06/06/2023 13:48	10
01_ped_bike	01_night	03_fog	10	02_lights_off	10m.bag	06/06/2023 13:42	9
01_ped_bike	01_night	03_fog	10	02_lights_off	19m.bag	06/06/2023 13:45	11
01_ped_bike	01_night	03_fog	10	02_lights_off	28m.bag	06/06/2023 13:48	10
01_ped_bike	01_night	03_fog	20	01_lights_on	10m.bag	06/06/2023 14:06	20
01_ped_bike	01_night	03_fog	20	01_lights_on	19m.bag	06/06/2023 14:00	21
01_ped_bike	01_night	03_fog	20	01_lights_on	28m.bag	06/06/2023 13:57	20
01_ped_bike	01_night	03_fog	20	02_lights_off	10m.bag	06/06/2023 14:07	20
01_ped_bike	01_night	03_fog	20	02_lights_off	19m.bag	06/06/2023 14:01	19
01_ped_bike	01_night	03_fog	20	02_lights_off	28m.bag	06/06/2023 13:57	20
01_ped_bike	01_night	03_fog	30	01_lights_on	10m.bag	06/06/2023 15:10	30
01_ped_bike	01_night	03_fog	30	01_lights_on	19m.bag	06/06/2023 15:06	28
01_ped_bike	01_night	03_fog	30	01_lights_on	28m.bag	06/06/2023 14:58	28
01_ped_bike	01_night	03_fog	30	02_lights_off	10m.bag	06/06/2023 15:10	28
01_ped_bike	01_night	03_fog	30	02_lights_off	19m.bag	06/06/2023 15:05	30
01_ped_bike	01_night	03_fog	30	02_lights_off	28m.bag	06/06/2023 15:02	30
01_ped_bike	01_night	03_fog	50	01_lights_on	10m.bag	06/06/2023 15:14	51
01_ped_bike	01_night	03_fog	50	01_lights_on	19m.bag	06/06/2023 15:17	52
01_ped_bike	01_night	03_fog	50	01_lights_on	28m.bag	06/06/2023 15:24	53
01_ped_bike	01_night	03_fog	50	02_lights_off	10m.bag	06/06/2023 15:15	52
01_ped_bike	01_night	03_fog	50	02_lights_off	19m.bag	06/06/2023 15:19	40
01_ped_bike	01_night	03_fog	50	02_lights_off	28m.bag	06/06/2023 15:25	55
01_ped_bike	02_day	03_fog	10		15m.bag	07/06/2023 09:33	11
01_ped_bike	02_day	03_fog	20		15m.bag	07/06/2023 09:42	20
01_ped_bike	02_day	03_fog	30		15m.bag	07/06/2023 09:45	31
01_ped_bike	02_day	03_fog	50		15m.bag	07/06/2023 09:57	54
03_car	01_night	03_fog	10	01_lights_on	10m.bag	06/06/2023 09:12	12
03_car	01_night	03_fog	10	01_lights_on	19m.bag	06/06/2023 08:44	11
03_car	01_night	03_fog	10	01_lights_on	28m.bag	05/06/2023 17:15	8
03_car	01_night	03_fog	10	02_lights_off	10m.bag	06/06/2023 09:12	12
03_car	01_night	03_fog	10	02_lights_off	19m.bag	06/06/2023 08:45	13

03_car	01_night	03_fog	10	02_lights_off	28m.bag	05/06/2023 17:15	11
03_car	01_night	03_fog	10		28m.bag	05/06/2023 17:01	12
03_car	01_night	03_fog	20	01_lights_on	10m.bag	06/06/2023 09:07	22
03_car	01_night	03_fog	20	01_lights_on	19m.bag	06/06/2023 08:48	20
03_car	01_night	03_fog	20	01_lights_on	28m.bag	05/06/2023 17:06	21
03_car	01_night	03_fog	20	02_lights_off	10m.bag	06/06/2023 09:08	20
03_car	01_night	03_fog	20	02_lights_off	19m.bag	06/06/2023 08:49	20
03_car	01_night	03_fog	20	02_lights_off	28m.bag	05/06/2023 17:07	16
03_car	01_night	03_fog	30	01_lights_on	10m.bag	06/06/2023 09:03	27
03_car	01_night	03_fog	30	01_lights_on	19m.bag	06/06/2023 08:51	30
03_car	01_night	03_fog	30	01_lights_on	28m.bag	05/06/2023 17:22	25
03_car	01_night	03_fog	30	02_lights_off	10m.bag	06/06/2023 09:04	29
03_car	01_night	03_fog	30	02_lights_off	19m.bag	06/06/2023 08:52	28
03_car	01_night	03_fog	30	02_lights_off	28m.bag	05/06/2023 17:22	27
03_car	01_night	03_fog	50	01_lights_on	10m.bag	06/06/2023 09:00	48
03_car	01_night	03_fog	50	01_lights_on	19m.bag	06/06/2023 08:55	48
03_car	01_night	03_fog	50	01_lights_on	28m.bag	05/06/2023 17:29	43
03_car	01_night	03_fog	50	02_lights_off	10m.bag	06/06/2023 09:01	53
03_car	01_night	03_fog	50	02_lights_off	19m.bag	06/06/2023 08:56	51
03_car	01_night	03_fog	50	02_lights_off	28m.bag	05/06/2023 17:29	44
03_car	02_day	03_fog	10		10m.bag	06/06/2023 09:42	11
03_car	02_day	03_fog	10		15m.bag	07/06/2023 10:12	10
03_car	02_day	03_fog	20		10m.bag	06/06/2023 09:46	19
03_car	02_day	03_fog	20		15m.bag	07/06/2023 10:15	20
03_car	02_day	03_fog	30		10m.bag	06/06/2023 09:49	27
03_car	02_day	03_fog	30		15m.bag	07/06/2023 10:18	32
03_car	02_day	03_fog	50		10m.bag	06/06/2023 09:51	49
03_car	02_day	03_fog	50		15m.bag	07/06/2023 10:21	53
04_targets	01_night	03_fog	10	01_lights_on	10m.bag	06/06/2023 14:32	10
04_targets	01_night	03_fog	10	01_lights_on	19m.bag	06/06/2023 14:29	8
04_targets	01_night	03_fog	10	01_lights_on	28m.bag	06/06/2023 13:30	10
04_targets	01_night	03_fog	10	02_lights_off	10m.bag	06/06/2023 14:32	9
04_targets	01_night	03_fog	10	02_lights_off	19m.bag	06/06/2023 14:30	8
04_targets	01_night	03_fog	10	02_lights_off	28m.bag	06/06/2023 13:31	9
04_targets	01_night	03_fog	20	01_lights_on	10m.bag	06/06/2023 14:12	19
04_targets	01_night	03_fog	20	01_lights_on	19m.bag	06/06/2023 14:16	19
04_targets	01_night	03_fog	20	01_lights_on	28m.bag	06/06/2023 14:26	19

04_targets	01_night	03_fog	20	02_lights_off	10m.bag	06/06/2023 14:12	19
04_targets	01_night	03_fog	20	02_lights_off	19m.bag	06/06/2023 14:17	20
04_targets	01_night	03_fog	20	02_lights_off	28m.bag	06/06/2023 14:26	18
04_targets	01_night	03_fog	30	01_lights_on	10m.bag	06/06/2023 14:43	29
04_targets	01_night	03_fog	30	01_lights_on	19m.bag	06/06/2023 14:48	31
04_targets	01_night	03_fog	30	01_lights_on	28m.bag	06/06/2023 14:52	30
04_targets	01_night	03_fog	30	02_lights_off	10m.bag	06/06/2023 14:43	28
04_targets	01_night	03_fog	30	02_lights_off	19m.bag	06/06/2023 14:49	25
04_targets	01_night	03_fog	30	02_lights_off	28m.bag	06/06/2023 14:53	28
04_targets	01_night	03_fog	50	01_lights_on	10m.bag	06/06/2023 15:41	58
04_targets	01_night	03_fog	50	01_lights_on	19m.bag	06/06/2023 15:35	55
04_targets	01_night	03_fog	50	01_lights_on	28m.bag	06/06/2023 15:29	53
04_targets	01_night	03_fog	50	02_lights_off	10m.bag	06/06/2023 15:41	56
04_targets	01_night	03_fog	50	02_lights_off	19m.bag	06/06/2023 15:36	53
04_targets	01_night	03_fog	50	02_lights_off	28m.bag	06/06/2023 15:30	49
04_targets	02_day	03_fog	10		15m.bag	07/06/2023 09:36	12
04_targets	02_day	03_fog	20		15m.bag	07/06/2023 09:39	20
04_targets	02_day	03_fog	30		15m.bag	07/06/2023 09:50	29
04_targets	02_day	03_fog	50		15m.bag	07/06/2023 09:52	49